Graduate School ETD Form 9
(Revised 12/07)

PURDUE UNIVERSITY
GRADUATE SCHOOL
Thesis/Dissertation Acceptance

This is to certify that the thesis/dissertation prepared

By Scott R. Hudson

Entitled Meckelin 3 is Necessary for Photoreceptor Outer Segment Development

For the degree of Master of Science

Is approved by the final examining committee:

Teri L. Belecky-Adams
Chair

Vince Gattone II

Bonnie Blazer-Yost

To the best of my knowledge and as understood by the student in the *Research Integrity and Copyright Disclaimer (Graduate School Form 20)*, this thesis/dissertation adheres to the provisions of Purdue University's "Policy on Integrity in Research" and the use of copyrighted material.

Approved by Major Professor(s): Teri L. Belecky-Adams

Approved by: Simon Atkinson 06/09/2011
Head of the Graduate Program Date

Graduate School Form 20
(Revised 9/10)

PURDUE UNIVERSITY
GRADUATE SCHOOL

Research Integrity and Copyright Disclaimer

Title of Thesis/Dissertation:

Meckelin 3 is Necessary for Photoreceptor Outer Segment Development

For the degree of Master of Science

I certify that in the preparation of this thesis, I have observed the provisions of *Purdue University Executive Memorandum No. C-22,* September 6, 1991, *Policy on Integrity in Research.**

Further, I certify that this work is free of plagiarism and all materials appearing in this thesis/dissertation have been properly quoted and attributed.

I certify that all copyrighted material incorporated into this thesis/dissertation is in compliance with the United States' copyright law and that I have received written permission from the copyright owners for my use of their work, which is beyond the scope of the law. I agree to indemnify and save harmless Purdue University from any and all claims that may be asserted or that may arise from any copyright violation.

Scott R. Hudson

Printed Name and Signature of Candidate

06/09/2011

Date (month/day/year)

*Located at http://www.purdue.edu/policies/pages/teach_res_outreach/c_22.html

MECKELIN 3 IS NECESSARY FOR PHOTORECEPTOR OUTER SEGMENT DEVELOPMENT

A Thesis

Submitted to the Faculty

of

Purdue University

by

Scott R. Hudson

In Partial Fulfillment of the

Requirements for the Degree

of

Master of Science

August 2011

Purdue University

Indianapolis, Indiana

ACKNOWLEDGMENTS

I would like to thank my committee members, Bonnie Blazer-Yost and Vince Gattone, for all their wisdom and guidance on my thesis project. To all the past and current lab members, your assistance, encouragement, and friendship throughout my graduate experience has been greatly appreciated. I would like to thank my advisor, Teri-Belecky-Adams, for allowing me the opportunity to continue towards my goal of becoming a scientist and for the invaluable graduate experience that has not only made me a better researcher, but a person as well.

TABLE OF CONTENTS

Page

LIST OF TABLES

LIST OF FIGURES

Figure Page

LIST OF ABBREVIATIONS

Autosomal Recessive Polycystic Kidney Disease	ARPKD
Bardet-Biedl Syndrome	BBS
Celsius	C
Centrosomal Protein	CEP
Embryonic day 9	E9
Frizzled	FZD
Ganglion Cell Layer	GCL
Glial Fibrillary Acidic Protein	GFAP
Hematoxylin and Eosin	H&E
Intraflagellar Transport	IFT
Inner Nuclear Layer	INL
Joubert Syndrome	JBTS
Kilograms	kg
Liter	L
Meckel-Gruber Syndrome	MKS
Microliter	ul
Microgram	ug
Microliter	um

Milligrams	mg
Milliliters	mL
Molar	M
Nanometer	nM
Nephronophthisis	NPHP
Outer Nuclear Layer	ONL
Optimal Cutting Temperature	OCT
Outer Segment	OS
Peroxidase-Anti-Peroxidase	PAP
Phosphate Buffer	PBS
Postnatal day 10	P10
Polycystic Kidney Disease	PKD
Retinal Pigmented Epithelium	RPE
Terminal deoxynucleotidyl transferase dUTP nick end labeling	TUNEL
Transmission Electron Microscopy	TEM
Units	U
Wild-type	WT
Wistar Polycystic Kidney	WPK

ABSTRACT

Hudson, Scott R. M.S., Purdue University, August 2011. Meckelin 3 is Necessary for Photoreceptor Outer Segment Development. Major Professor: Teri L. Belecky-Adams.

Ciliopathies with multiorgan pathology include renal cysts and eye pathology. Retinal photoreceptors have connecting cilia joining the inner and outer segment that are responsible for transport of molecules to develop and maintain the outer segment process. The present study evaluated meckelin expression during normal postnatal retinal development and the consequences of mutant meckelin on photoreceptor development and survival in Wistar polycystic kidney disease Wpk/Wpk rat using immunohistochemistry, analysis of cell death and electron microscopy.

Meckelin was co-expressed in the inner and outer segments of photoreceptor rods and cones, amacrine, Muller glia and ganglion cells in postnatal day 10 (P10), P21 and mature rat retinae. By P10, both the wild type and homozygous Wpk mutant retina had all retinal cell types. In contrast, by P21, cells expressing photoreceptor-specific markers were fewer in rhodopsin, long/medium-wave opsin, and short-wave opsin proteins and appeared to be abnormally localized to the cell body. Cell death analyses were consistent with the disappearance of photoreceptor-specific markers and showed that the cells were undergoing caspase-dependent cell death. By electron microscopy, mutant photoreceptors did not develop an outer segment process beyond a connecting cilium and

rudimentary outer segment. We conclude that MKS3 is not important for formation of connecting cilium and rudimentary outer segments (the inner stripe), but is critical for the development of mature outer segment processes. The meckelin mutants showed similarities to human patients suffering from Leber's congenital amaurosis. We propose this may be a useful model system for studying early photoreceptor degeneration diseases such as Leber's congenital amourosis.

CHAPTER 1. INTRODUCTION

Eye Development

Early mammalian embryos go through a process called gastrulation that will produce three germ layers (mesoderm, endoderm and ectoderm) [1]. On the dorsal side of the embryo, neurulation starts with the formation of the neural plate from ectoderm (Figure 1.1). The neural plate folds up and undergoes closure to form the neural plate [2]. During early embryonic stages, the first overt sign of eye development is the formation of the optic pits in the diencephalic region of the forebrain. Upon completion of neural tube closure, the optic pits enlarge and continue to evaginate to become optic vesicles. The optic vesicles are located close to the non-neuronal surface ectoderm and it has clearly been shown that inductive signaling occurs between the two [3]. This signaling gives rise to the lens placode. Together, the optic vesicles and lens placode invaginate to form the optic cup and lens vesicle, respectively (Figure 1.1). The inner part of the optic cup will give rise to the multi-layered neural retina and the outer part will make up the single layered retinal pigmented epithelium (RPE) [4].

In early retina morphogenesis, there are many different transcription and secreted factors that play significant roles. The formation of the optic vesicle relies upon specific molecular mechanisms that start prior to the formation of the optic pits. The anterior neural plate cells express *Pax6*, *Pax2*, and *Rx*, denoting what is referred to as the eye field

[4]. The eye field is localized in the center of the diencephalic region of the neural tube. For the development of two vertebrate eyes, the eye field must be split into two regions. This is accomplished through the establishment of the floorplate in the midline of the eye field. The floorplate arises through the induction of a nearby structure, known as the prechordal plate, which expresses a molecule known as sonic hedgehog (SHH). As this factor interacts with the neural plate, it up-regulates molecules necessary for eye field formation [5]. This inductive event causes what was one eye field to become two. These two regions then move laterally and form the optic pits as discussed above. Once the eye field splits and neural tube undergoes closure, the optic vesicles will form. *Mitf*, microphthalmia-associated transcription factor, is initially expressed throughout the optic vesicle, but its expression becomes restricted to the proximal region of the optic vesicle responsible for the retinal pigmented epithelium (RPE) [6]. *Chx10*, a paired-like homeobox gene, is necessary for the differentiation of the retina and is induced as the optic vesicle comes in close contact with the head ectoderm. The head ectoderm expresses FGF2 which is necessary and sufficient to induce expression of CHX10. CHX10 is initially expressed throughout the neural retina and plays a role in proliferation in the early neural retina [7]. Later in development, the expression of CHX10 is reduced to inner nuclear layer (INL) and is responsible for the differentiation of bipolar cells [8].

Mature Retinal Anatomy and Physiology

The vertebrate retina is a multi-layered tissue consisting of cell bodies in the retinal pigmented epithelium (RPE), outer, inner, and ganglion cell layers (Figure 1.2). The retina also has outer and inner plexiform layers where cells from different layers can

form synapses. The outer nuclear layer (ONL) contains the cell bodies of 2 type of photoreceptors; rods and cones. The inner nuclear layer contains the cell bodies of horizontal, bipolar, Muller glial and amacrine cells (Figure 1.2). The ganglion cell layer contains ganglion cells and a subset of amacrine cells. Retinal cell types come from progenitor cells that can differentiate into all retinal cell types [9]. Retinal cell genesis was previously studied in the rat to obtain a better understanding of precisely when each retinal cell type is first generated [10]. The following is the order from earliest to latest of each generated retinal cell type: ganglion, horizontal, photoreceptor cone, amacrine, photoreceptor rod, Muller glial and bipolar [11]. All cell types start to form during the embryonic stages with ganglion cells starting the earliest at embryonic day 9 (E9) [12]. The ganglion, horizontal and photoreceptor cone cells finish developing during embryonic stages; however, the amacrine, photoreceptor rod, Muller glia and bipolar cells conclude their cell genesis shortly after birth [10].

The main function of the retina is to turn absorbed light into a biological signal through a process known as phototransduction [13]. This biological signal is in the form of an electrical hyper-polarization of the cell membrane and controls the rate at which glutamate, a neurotransmitter, is released from the photoreceptor synaptic terminal. Photoreceptor outer segments have cyclic GMP (cGMP)-gated ion channels on the plasma membrane that open and close depending on whether it is dark or light out (Figure 1.3). During darkness, the cGMP-gated ion channels are open and allow Na^+ and Ca^{2+} to enter the outer segment[14]. Entrance of Na^+ and Ca^{2+} will depolarize the cell, activating the voltage-gated Ca^{2+} channels near the synaptic terminals of the photoreceptors, and will drive the release of glutamate from the synaptic terminal. In the

presence of light, visual pigment in stacked discs in the outer segment will absorb light (Figure 1.3 [15]). The absorbed light will cause retinal, a derivative of Vitamin A, to undergo a conformational change to opsin and all-trans-retinal [16]. Opsin will proceed to activate the trimeric G-protein transducin, causing the α subunit to be released from the β and γ subunits and exchange GDP for GTP. This GTP complex will activate phosphodiesterase, which subsequently breaks down cGMP to 5'-GMP [13]. This breakdown will lower cGMP concentration, which in turn closes the cGMP-gated ionic channels. Closure of sodium channels will cause the cell to hyperpolarize and the voltage-gated Ca^{2+} channels to close. This will result in a decrease in the amount of glutamate released from the synaptic region of photoreceptors [13,14,16].

Photoreceptors make synapses with both bipolar and horizontal cells in the outer plexiform layer of the retina. Photoreceptor can have synapses with bipolar cells that can either be considered on- or off-center (Figure 1.4). An on-center bipolar cell is stimulated when the center of its receptive field is exposed to light and inhibited when light hits the surrounding area. The off-center bipolar cells have an opposite reaction of being inhibited with direct light to the center and excited when light is exposed in the surrounding area of the receptor field [17]. When light is present, photoreceptors hyperpolarize and on-center cells depolarize. Horizontal cells link photoreceptors to each other and are responsible for lateral inhibition of photoreceptors [18]. Photoreceptors will then depolarize horizontal cells in order for them to depolarize photoreceptors that are not in the region of excitation, resulting in lateral inhibition [19]. The overall result of this lateral inhibition is to increase the signal in relation to the background activity present in the nervous system. Ganglion cells will then receive input from bipolar and

amacrine cells from synapses formed in the inner plexiform layer (IPL). Ganglion cells also have on- and off-center cells that function in a similar fashion as bipolar cells [20]. Amacrine cells function in a similar manner as horizontal cells in that they also appear to be necessary for lateral inhibition. They differ from horizontal cells in that they relay information from bipolar cells to ganglion cells. Ganglion cells project their axons to the optic nerve head, where the axons are bundled together to form the optic nerve [21]. Neuronal signals travel out of eyes and goes to one of three places; 1) the pretectum, where light signals maintain the pupillary light reflex, 2) the superior colliculus (aka tectum), which is involved in reflexive eye and head movements in response to visual stimuli, and 3) the lateral geniculate nucleus of the thalamus, which acts as a relay station for information that will be sent on to the cortex [22] (Figure 1.5 [23]).

Vertebrate Photoreceptor Development

Photoreceptors can be broken down into two different cell types; rods and cones. Photoreceptors develop from a pool of dividing progenitor cells in the vertebrate retina. There are several known transcription factors that previous studies have found important for photoreceptor development. Otx2, an Otx-like homeobox gene, has been found to be essential for cell fate determination for photoreceptor cell types. In a previous studies, a switch from photoreceptor precursor cells to amacrine cells were observed in otx2 knockout mice [24,25]. Crx, a cone-rod homeobox gene, has been found essential for terminal differentiation of rods and cones by regulating genes encoding phototransduction, photoreceptor metabolism, and outer segment formation [25,26,27]. Nrl, neural retina leucine zipper gene, is a transcription factor mainly found in rods and

promotes rod development by directly activating rod-specific genes while also suppressing S-cone related genes. S-cone related genes can be suppressed through the activation of transcriptional repressor nuclear receptor subfamily 2 group E member 3 (Nr2e3) [25,28]. Finally, neuroD, a member of the family of proneural basic helix-loop-helix genes, is found first in proliferating cells that give rise to rod and cone photoreceptors and is subsequently restricted to post mitotic cells of nascent cone photoreceptors [29,30].

As photoreceptors differentiate, they form 4 specialized compartments (Figure 1.6); 1) the outer segment, specialized for transduction of photons, 2) the inner segment containing machinery for producing proteins, lipids, and energy, 3) the nuclear region, and 4) the synaptic region, necessary for communicating with horizontal and bipolar cells within the retina [31]. Because of this compartmentalization, the sorting of proteins and other components to the right compartment is a highly regulated process in photoreceptors [32].

While photoreceptor rod and cone cells are similar in structure, they have differences in function. Rod cells outnumber cone cells by far in humans (approximately 120 million to 6 million) and are more common in the peripheral retina, while cones are more common in the center. Rod cells are highly sensitive to light and are specialized for night vision. Rod cells only have one visual pigment, rhodopsin. Cone cells are less sensitive to light and are more specialized for day time vision [33]. Also, cone cells are responsible for the fine detail and color vision. Cone cells also come in three different types: long (red), medium (green), and short (blue) wavelengths. Having three different cone cell types allows the brain to perceive a broad spectrum of colors.

The inner and outer segments of photoreceptor cells are joined by a modified non-motile connecting cilium through which essential elements are transported for outer segment morphogenesis (Figure 1.7). The connecting cilia in the photoreceptor is a "9+0" primary cilia that has nine microtubule doublets without a central pair [14]. The central core of the cilium is held in place by this microtubule backbone called an axoneme. This axoneme is anchored in the inner segment of the photoreceptor to a basal body. The primary function of the basal body is to act as the organizing center for the cilia [34]. The connecting cilium uses a specialized system called intraflagellar transport (IFT) as a pathway for the transport of proteins to and from the outer segment (Figure 1.8). In this transport process, the cilia uses the motor protein kinesin to move cargo from inner to outer segment and the motor protein dynein to move components back to the cell body [35]. While much information has been accumulated about the photoreceptors, there still remain many questions about the mechanisms of outer segment formation, protein transport through the connecting cilium, and the implications of alterations in protein trafficking to diseases affecting outer segment development and/or maintenance.

Outer Segment Development

Photoreceptor cell genesis has been well studied; however, the formation of outer segment discs is still not well understood. The first proposed theory suggests that the plasma membrane invaginates to form disc-like structures [36]. As the connecting cilium extends, the plasma membrane forms a balloon-like structure around the connecting cilium, followed by the invagination of the plasma membrane to form discs (Figure 1.9).

The second theory proposes that disc formation is due to pinocytosis of smaller vesicles that then fuse together to form a full disc that connects at the base of the outer segment, compressed by unknown mechanisms and then stacked together (Figure 1.10) [37]. Disc formation is not limited to initial outer segment development, as it is continued all the through adulthood (Figure 1.11 [36]). Each day, the photoreceptor will shed $1/10^{th}$ of its total discs on the distal most tip and that will get phagocytized by the retinal pigmented epithelium. With either theory, the newly formed discs receive visual pigment that was made in the inner segment and transported to the outer segment through IFT. Photoreceptors with mature outer segments can now take part in their main function of phototransduction.

Ciliopathies of the Retina

Nearly all vertebrate cells contain microtubule-based structures known as cilia. Cilia are anchored into the cell by the basal body and have microtubule doublets extending away from the cell surface. The function of the cilia depends on its structure. Motile cilia have nine microtubule doublets in a circular pattern with an extra pair in the center (9 + 2) and serve the function of movement. Non-motile, or primary cilia, have only the nine microtubule doublets without the center pair (9 + 0) and their main function is to be a sensory organelle [38]. While the full range of sensory organelle functions are not well understood, they participate in transforming extracellular signals to intracellular changes [39]. Cilia are located throughout the entire body and have important functions for many different organs. Previous studies have investigated several diseases associated with abnormal cilia structure and/or function and are now known as ciliopathies.

Ciliopathies are caused by genetic mutations containing defective proteins. To date, over 40 genes have been identified with ciliopathic diseases [40]. Ciliopathies have been identified in multiple organs including kidneys, thyroid gland, liver, pancreas and eye, as well as multiple cell types including endothelial cells, the myocardium, odontoblasts, photoreceptors, and cortical and hypothalamic neurons [41]. Phenotypes tend to overlap within the different syndromes classified as ciliopathies and a list phenotypes from well studied ciliopathies are found in Table 2 [40]. The vertebrate eye contains primary cilia in photoreceptor cell types that are involved in the outer segment development and maintenance. Proper outer segment formation is crucial for photoreceptors to participate in phototransduction in order to allow for vision. Eye diseases that are caused by irregular primary cilia in photoreceptors are known as retinal ciliopathies.

Retinal ciliopathies include several photoreceptor degenerative diseases that involve certain genes that play an important role in ciliogenisis and/or protein transport to the cilium [42]. For phototransduction to occur properly, visual pigment made in the inner segment of photoreceptors has to be transported to the outer segment. Failure to do so results in an accumulation of visual pigment in the inner segment and ultimately leads to photoreceptor cell death. Retinal ciliopathies have several known genes that are associated with ciliary function that include: Retinitis Pigmentosa-1 (RP-1), Retinitis Pigmentosa GTPase Regulator (RPGR), Retinitis Pigmentosa GTPase Regulator Interacting Protein (RPGR-IP), Usher (USH), Nephronophthisis (NPHP) and Bardet-Biedl (BBS) [34]. Ciliopathies in general can be single organ disorders or multisystemic disorders affecting multiple organs in the body. For example, the RPGR gene is known to located in the photoreceptor connecting cilium and be involved with

protein transport and morphogenesis. Some mutations in RPGR lead to the eye disease retinitis pigmentosa, however, some mutations with RPGR lead to systemic malformations like primary cilia dyskinesia [42]. Primary cilia dyskinesia is a genetic disorder affecting the motility of cilia that causes chronic destruction in the respiratory system, randomization of left-right body asymmetry and reproduction system defects [43].

Meckel-Gruber Syndrome and Models of Meckel-Gruber

Ciliopathies are a group of genetic disorders characterized by mutations in proteins found in the primary cilia [44]. Included in this category are syndromes such as; polycystic kidney disease (PKD), Bardet-Biedl (BBS), nephronophthisis (NPHP), Alstrom, and Meckel-Gruber Syndrome (MKS). MKS is a rare, autosomal recessive, lethal, ciliopathic, genetic disorder characterized by renal cystic dysplasia, and central nervous system malformations, but can also be associated with situs inversus, polydactyly and hepatic developmental defects [45]. MKS has a worldwide incidence that varies from 1/13,250 to 1/140,000 live births with males and females affected equally [46]. This deadly disease can be diagnosed prenatally during ultrasonographic screening for fetal chromosomal abnormalities. Depending on the gestational age, the sonograph findings for MKS could include occipital encephalocele, postaxial polydactyly and cystic kidneys [47]. Once MKS is diagnosed, the mortality is 100%. Infants with MKS will either be stillborn or die a few hours after birth [45].

MKS or Meckel-like syndrome has been linked to ten genes that include: ***MKS1****/BBS13* [48], ***MKS2****/TMEM216/JBTS2* [49,50], ***MKS3****/TMEM67/JBTS6* [51],

MKS4*/CEP290/NPHP6/JBTS5/BBS14* [52], ***MKS5****/RPGRIP1L/CORS3/NPHP8/JBTS7* [53] and ***MKS6****/CC2D2A* [54]. In addition, other proteins unrelated to the Meckelin family of proteins have also been associate with a Meckel-like syndrome, including *NPHP3, BBS2, BBS4* and *BBS6* [55,56]. These proteins are all associated with either the basal body or the cilium. The MKS3 gene for meckelin is one of the first to be associated with the Meckel-Gruber syndrome and is widely expressed in all tested human tissue [57]. Previous work has suggested that this gene may be critical to cilia function in kidney, liver, and retina. [58].

Meckelin and Related Proteins

Meckelin, the *MKS3* gene protein product, comprises of 995 amino acids in human and mouse and 997 amino acids in rat. Previous studies have shown that human and rat meckelin are 84% identical and 91% similar [57]. The predicted structure of meckelin consists of a seven transmembrane region and a short cytoplasmic tail [59]. This protein structure is similar to those of the Frizzled (FZD) family of receptor proteins, suggesting that meckelin could play a role as a receptor. Also, it is known that the MKS3 promoter sequence has an X-box motif that has previously been found to take part in the regulation of primary ciliary genes in C. elegans [57,59]. With the acquired knowledge of the meckelin's structure, the role of similarly structured proteins, and the phenotype of humans and animals carrying mutations, we postulate that meckelin plays an important role in primary cilia function.

In this study, the expression patterns of meckelin have been studied using immunohistochemistry in the developing and mature rat retina. Using the Wistar-Wpk

rat with a spontaneous mutation in the *rMks3* gene [57], we previously showed that the formation of the photoreceptor outer segment development was dramatically impaired leading to loss of the photoreceptors [58]. Herein, we found that the photoreceptors underwent rapid degeneration around three weeks of life following a brief period when many transduction proteins appear to be mislocalized to the inner segment, nuclear and synaptic regions. Since a connecting cilium was present, we hypothesize that meckelin may not be important for connecting cilium formation and rudimentary outer segment formation, but may be critical for the maturation and maintenance of the outer segment process.

CHAPTER 2. EXPERIMENTAL PROCEDURES

WPK Rat Model

Dr. Jeroen Nauta (Erasmus Medical Center Rotterdam, Rotterdam, Netherlands) provided heterozygous Wistar WPK breeders with Autosomal Recessive Polycystic Kidney Disease (ARPKD). A subcolony was established at the IU School of Medicine and all studies were performed with approval of the IU School of Medicine IACUC Approval (MD-3119). Animals were housed at the Indiana University School of Medicine Laboratory Animal Resource Center, and the initial litters were delivered via cesarean section in order to ensure that the line was pathogen-free [60]. Litters from the heterozygous WPK/+ crosses were sacrificed at 10 day and three weeks. Rats were anesthetized with sodium pentobarbital (100mg/kg administered i.p.), and then perfusion fixed with 4% paraformaldehyde in 0.1 M phosphate buffer (pH 7.4). Eyes were dissected free, rinsed twice in 1X phosphate buffered saline (PBS; potassium chloride 200 mg/L, potassium phosphate 200 mg/L, sodium chloride 8000 mg/L, and sodium phosphate 1150 mg/L), pH 7.5 and placed in 20% sucrose made in 0.1 M phosphate buffer overnight. Eyes were frozen in a 3:1 ratio of 20% sucrose in 0.1M phosphate buffer to Optimal Cutting Temperature (OCT) solution and stored at -80^{o}C.

Molecular and Cellular Techniques

Immunohistochemistry

Ten micron sections were cut with a Leica CM3050 S cryostat placed on Superfrost Plus slides (Fisher Scientific, Pittsburgh, PA) and stored at -80^{o}C until used for immunohistochemistry. Immunohistochemistry was performed as described previously [61]. Briefly, slides with tissues samples were removed from freezer and allowed to warm to room temperature for 10-15 minutes. Slides were then washed with 1X PBS twice for 10 minutes. Sections were circled using a PAP pen (Electron Mircroscopy Sciences, Hatfield, PA) followed by incubation for one hour at room temperature in 10% serum diluted in 1X PBS with 0.25% triton X-100. After removing blocking solution, sections were incubated overnight at 4^{o}C with the primary antibody diluted in PBS containing 2% serum (same serum as used in blocking) in PBS containing 0.025% triton X-100. Dilutions and sources of each antibody can be found in Table I. Then slides were warmed to room temperature for 10-15 minutes, followed by removal of primary antibody and washing with 1X PBS twice at room temperature for 10 minutes. Sections were then incubated for one hour at room temperature with alexa-fluora (Invitrogen, Eugene, OR) or DyLight (Jackson ImmunoResearch, West Grove, PA) conjugated secondary antibodies diluted to 1:800 in 1X PBS. Following secondary antibody, slides were washed twice in 1X PBS at room temperature for 10 minutes each rinse. Slides were then incubated for 2 minutes at room temperature with 0.9 M Hoechst dye (H6024, Sigma-Aldrich, St. Louis, MO), then rinsed briefly with 1X PBS at room temperature, and mounted using aqua poly/mount (Polysciences, Warrington, PA).

Slides were stored protected from light until analysis using a Nikon Eclipse E800 epifluorescence microscope equipped with a Nikon Digital Camera DXM 1200 or an Olympus Fluoview FV 1000 confocal.

TUNEL Labeling

Frozen tissues samples were allowed to warm to room temperature for 10-15 minutes and subjected to TUNEL labeling using an *In situ* cell death detection kit (Roche, Indianapolis, IN) as per manufacturer's instructions. Briefly, tissue sections were post-fixed with 4% paraformaldehyde, washed with 1X PBS for 30 minutes at room temperature and permeabilized with 0.1% Triton X-100, 0.1% sodium citrate in 1X PBS for 2 minutes on ice. Sections were then rinsed with 1X PBS, followed by incubation with TUNEL reaction mixture for 60 minutes at 37^{o}C in a humidified atmosphere in the dark. Slides were then rinsed 3 times with 1X PBS and mounted using an antifade agent (Prolong Gold, Invitrogen, Carlsbad, CA). Samples were analyzed using an Olympus confocal laser scanning microscope using an excitation wavelength of 488 nM. A negative control without addition of label solution and a positive control incubated with 3000 U/ml of DNAase I recombinant were also subjected to similar conditions and analyzed.

H&E Staining

Frozen tissues samples were allowed to warm to room temperature for 10-15 minutes and rinsed 2 times with 1X PBS. Sections were then stained with Harris hematoxylin solution (1x) for 8 minutes. Next, wash slides in running tap water for 5-10

minutes. Sections were then stained with eosin Y solution for 1 minute and dipped in water until the liquid runoff changed from color to clear. Slides were then dipped 10 times in 50, 70, 90 and 95% ethanol, respectively. Slides were dipped 5 times in xylene and mounted with Cytoseal-XYL, a xylene based mounting medium.

Transmission Electron Microscopy

Wpk rats were perfused through the left ventricle with 4% paraformaldehyde in 0.1 M phosphate buffer. Tissue sections used for electron microscopy were placed in 2% paraformaldehyde, 2% glutaraldehyde in phosphate buffer. Tissue was processed from TEM by the Electron Microscopy Center at the Indiana School of Medicine, Indianapolis using standard methods (http://anatomy.iupui.edu/core-facilities/electron-microscopy-center/). Briefly, tissue was cut into 1 x 2 mm segments, post-fixed in osmium tetroxide, dehydrated in a graded series of ethanol, infiltrated and embedded in Embed 812 (Electron Microscopy Sciences). Sections were cut with a diamond knife on a Leica UCT Ultramicrotome (Leica), stained with uranyl acetate and examined using a Tecnai G2 12 Bio Twin (FEI) [60].

Tissue Analysis and Statistics

Digital images for cell death (TUNEL and caspase 3), retinal cell layer thickness measurements (H+E stain) and retinal cell counts were taken by an Olympus Fluoview FV1000 confocal microscope. For cell death and retinal cell counts, positively labeled cells were counted over a 100µm area that was 200µm dorsal and ventral from the optic nerve. Similar to cell death and cell count assays, we measured retinal cell layer

thicknesses 200μm dorsal and ventral of the optic nerve using the FV10-ASW 2.1 Viewer software of the Olympus Fluoview FV1000 confocal microscope. To determine the significance of our data, we used an unpaired t-test that compared age-matched littermates of wild type (WT) and mutant rats (Graphpad Software, http://www.graphpad.com/quickcalcs/ttest1.cfm).

CHAPTER 3. RESULTS

Meckelin 3 is Found in the Developing and Mature Rat Retina

To initially determine if MKS3 might be important for photoreceptor outer segment formation and/or maintenance, the localization of MKS3 in the developing rat retina was examined. Cryosections through postnatal day 10 (P10), P21, and mature retinae were probed with an MKS3-specific antibody (See Figure 3.1). In the developing retina, expression of MKS3 was fairly widespread. At both P10 (Fig 3.1A-B) and P21 (Figure 3.1C-D) signal was detected in the outer nuclear layer, a subset of cells in the inner nuclear layer (INL) and the ganglion cell layer (GCL). In the mature retina, labeling was still apparent in the photoreceptor outer/inner segments as well as in the GCL (Figure 3.1E, F). Staining was no longer detectable in the INL.

MKS3 is known to interact with ciliary proteins in other cell types [62]. To examine the localization of meckelin in photoreceptors, we double-labeled cryosections through mature retina with antibodies against proteins known to be present in the axoneme of the photoreceptor outer segment. Acetylated microtubules are enriched in the photoreceptor axoneme [63] and appeared to co-localize with MKS3 in the mature outer segment (Figure 3.1G-I).

To further characterize expression patterns and determine which cell types expressed MKS3 in the mature retina, we performed double-label immunohistochemistry

using antibodies against specific retinal cell markers at P21. The expression of meckelin in rods and cones was first determined (Figure 3.2). MKS3 was clearly detected in both photoreceptor cell types labeled as seen in overlays of sections co-labeled for rhodopsin and meckelin (Figure 3.2F) or L/M opsin and meckelin (Figure 3.2L). MKS3 expression was also compared to other cells type-specific markers found in the inner and GCL, including calbindin (horizontal cells), Chx10 (bipolar cells), Sox2 (Muller glia and astrocytes), parvalbumin (amacrine cells), and Brn3a (ganglion cells). We detected no co-expression in cells that were positive for calbindin (Figure 3.3A-D) or Chx10 (Figure 3.3E-H). However, MKS3 was co-expressed in cells that were positive for Sox2 (Figure 3.3I-L) parvalbumin (Figure 3.3M-P) and Brn3a (Figure 3.3Q-T).

Histological Analysis of Retinae Isolated from Rat Mutant for Meckelin 3

To further test the hypothesis that MKS3 is critical for the formation of photoreceptor outer segments, we utilized a rat with a spontaneous autosomal recessive mutation of the *Mks3* gene, referred to as the rat Wistar polycystic kidney disease model (WPK; [64]). The progression of the polycystic kidney disease (PKD) has been well characterized in this strain of rats and culminates in a majority of the rats dying between 3 and 6 weeks of age [64,65], therefore we restricted our analysis of the WPK retinae to the early postnatal stages prior to stages when rats were extremely ill and/or dying. Previous work has shown that there were fewer photoreceptors in the rat WPK model than their wild type (WT) counterparts, however the cellular changes in photoreceptors during retinal development has not been fully characterized [58]. A histological analysis of retinal sections at postnatal days 10 and 21 was performed to determine the rate of

photoreceptor development in the WT and WPK littermates. Sections through the central retina of WT and mutant were stained with hematoxylin and eosin and the thickness of the outer (ONL), inner (INL), and ganglion cell (GCL) layers measured on digital images of the sections in regions dorsal and ventral to the optic nerve (see Materials and Methods for full description). Since there were no significant differences between dorsal and ventral measurements, the data from both were pooled together to obtain the histograms in Figure 3.4. At P10, there was no change in the thickness of the INL and GCL in WT and mutant retinae; however there appeared to be a change in thickness of the ONL in comparison to the WT counterparts (Figure 3.4A, B, E). There was a tendency for the ONL to be thinner in P10 mutant rats; but the difference was not statically significant. At P21, no statistically significant changes were noted in the mutant INL and GCL in comparison to the WT. In contrast, the ONL still showed significant reduction in the thickness of the mutant ONL in comparison to the WT (Figure 3.4C, D, F).

Cell Loss in the WPK Mutant Retinae

In the results above, MKS3 was clearly detected in photoreceptors and cells of the INL and GCL, and there appeared to be a loss of cells in the ONL layers. To further determine whether both rods and cones are lost in the WPK rat and whether other cells types in the INL and GCL were also affected by the MKS3 mutations, cryosections through control WT and mutant P21 eyes were analyzed using cell type-specific antibodies. Using antibodies against rhodopsin (rods), L/M opsin (cones), and S opsin (cones), it was apparent that both rods and cones were severely affected by the MKS3

mutation (Figure 3.4). In comparison to age-matched WT littermates, there appeared to be a significant reduction in the number of labeled rods at P21 (Figure 3.4G-J). Further, immunolabeling for the L/M opsin in mutant retinae revealed mislocalization of the opsins to cell bodies in comparison to the WT control which showed labeling in the inner and outer segment (Figure 3.4K-N). Very few cells were S opsin-positive in the WT retina (Figure 3.4O-P) and none could be found in the WPK mutant (Figure 3.4Q-R).

To detect cells in the INL and GCL, we immunolabeled P10 and P21 cryosections with calbindin for horizontal cells, Chx10 for bipolar cells, Sox2 for Muller glia and astrocytes, parvalbumin for amacrine cells and Brn3a for ganglion cells. At P10, expression patterns of calbindin, Chx10, Sox2, parvalbumin, and Brn3a all appeared similar in WT and mutant retinae. At P21, expression patterns of calbindin (Figure 3.5A-D), Chx10 (Figure 3.5E-H), and Sox2 cells (Figure 3.5I-L) were similar in WT and WPK mutant retinae. Parvalbumin expression was found similarly within the INL of both the WT and WPK mutant retina (Figure 3.5M-P). However, a significant amount of parvalbumin expression was found in the GCL of WPK mutants in comparison to their WT counterparts (Figure 3.5M-P). Brn3a expression appeared similar in the WT and mutant retinae (Figure 3.5Q-T). At P21, we also immunolabeled WT and mutant retinal sections with glial fibrillary acidic protein (GFAP) to detect reactive glia present in degenerating retinae. A small amount of GFAP expression was localized to the endfeet in WT retinae (Figure 3.5U-V); however, a significant increase of GFAP occurred throughout the cell body of Muller glia in the mutant (Figure 3.5W-X).

To confirm that there was only a loss of rods and cones in the mutant retinae, it was necessary to perform cell counts for each retinal cell type at P10 and P21. At P10,

cell counts comparing WT to mutant for all retinal cell types were all similar in number with no significant differences, including photoreceptor cell types (Figure 3.8A). This is consistent with our previous immunostaining and suggests that all retinal cell types are initially present in the Wpk mutant rat. Analyses of P21 retinal cell counts confirmed that both photoreceptor rod and cone cell types were the only retinal cell types to be significantly reduced (Figure 3.8B). These results confirm that the Wpk mutant rat undergoes photoreceptor degeneration between P10 and P21.

To further analyze the apparent decrease in photoreceptors in the WPK mutants, we labeled sections through central retina with the terminal deoxynucleotidyl transferase mediated dUTP nick-end-labeling (TUNEL) assay or with an antibody against caspase 3 to detect cells undergoing apoptosis. At P10, there were very few cells labeled with TUNEL or caspase 3 in the INL and GCL of the WT or mutant retinae (Figure 3.6I, J). Similarly, at P21 there were also very few positive cells in the INL and GCL of both the WT and mutant retinae. Consistent with the measurement data, however, at P10 there was a small but statistically significant increase in caspase 3- labeled cells in the mutant ONL in comparison to the WT (Figure 3.6J). However, WT and mutant ONL at P21 were strikingly different. While the P21 ONL of WT retinae had virtually no cells labeled for TUNEL or caspase 3, the mutant rats had an abundance of TUNEL- and caspase 3-labeled cells (Figure 3.6I, J).

Rudimentary Outer Segments are Initiated Prior to Photoreceptor Degeneration in the WPK Mutant

In the WT rat model, photoreceptors begin to develop before birth and fully mature by 3 weeks [10]. To determine if photoreceptor outer segments initially form in the WPK rat, transmission electron microscopy (TEM) images were compared in the control WT retina and the WPK rat retina. High resolution TEM images show inner and outer segment formation at P10 and P21 in WT and WPK rats (Figure 3.7). At P10, rods in the WT retinae were just beginning to form outer segments accompanied by laminated discs (Figure 3.7A inset). However, the WPK mutant photoreceptor cilia form bulbus terminae without the formation of discs (Figure 3.7B with inset). By P21, the WT retinae have completed outer segment formation with numerous laminated discs (Figure 3.7C with inset). However, in the retinae of mutant rats lack outer segments with the cilia projecting into a loosely organized area without evidence of laminated discs (Figure 3.7D with inset).

CHAPTER 4. CONCLUSION

Summary of Findings

In this study, we have investigated the normal expression patterns of the MKS3 protein in the developing rat retina and tested its role in outer segment formation. The following summarizes our findings: 1) MKS3 was found in photoreceptors as well as amacrine, Muller glial, and ganglion cells in the developing rat retina, 2) MKS3 was restricted to the ONL and GCL of the mature rat retina, 3) rats with a naturally occurring point mutation in the *Mks3* gene showed a loss in the thickness of the ONL as well as an apparent loss in the number of cells labeled with rod and cone-specific markers in the WPK mutant rat in comparison to the WT, 4) the loss of outer segments in photoreceptors was linked to an increase in apoptosis, and 5) EM data showed that WT and WPK photoreceptors developed an axoneme on the same time scale; however Mks3 mutant rats were only able to produce rudimentary outer segment. We conclude from these studies that the MKS3 protein product is essential for the development of the outer segment in both rods and cones and the absence of the outer segment process leads to apoptosis of the developing rods and cones.

Photoreceptor Outer Segment Development and Meckelin 3

The outer segment of the photoreceptor is initially developed as an extension of the connecting cilium. The basal side of the connecting cilium is anchored in the inner segment by the basal body and its apical side elongates to form the start of the outer segment. The stacked discs of the outer segment that house the visual pigments necessary for phototransduction are formed through a process that is still somewhat controversial. The discs arise from either the evagination of the plasma membrane from the base of the connecting cilia or the fusion and compression of pinocytic vesicles that arise from the plasma membrane [36,37,66,67,68]. In vertebrate rod cells, these disk membranes pinch off and separate, while in cone cells they are continuous with the plasma membrane. This outer segment disk formation is continued throughout adulthood due to the daily shedding of the discs from the most apical end of the OS [42]. In the studies presented here, rudimentary rod photoreceptor outer segments consisting of the connecting cilium and plasma membrane were present. However, no further outer segment development was noted.

Cell Death in *Mks*3 Mutants

There was substantial cell death associated with photoreceptors in the MKS3 mutant rat by postnatal day 21. Photoreceptor death appears to be a consistent theme in animal studies as well as in human diseases involving retinal disease [69,70,71,72]. Photoreceptors appear to preferentially use the caspase-dependent apoptotic pathway during degeneration [73]. We initially tested for cell death using the TUNEL assay, which is a non-specific marker of cell death occurring by apoptotic as well as necrotic

and autolytic pathways [74,75]. We subsequently showed using the localization of a member of the apoptotic pathway, caspase 3, that the photoreceptors in the mutant rat were using the caspase-dependent pathway [76,77]. There are a number of hypotheses proposed which may give us clues as to why these photoreceptors undergo apoptosis [73]. One hypothesis attributes photoreceptor death in other model systems to hyperoxic conditions that arise as a result of a decrease in phototransduction that would occur if outer segments do not form and therefore transduction of light does not take place. The process of phototransduction relies on high levels of oxygen consumption, and the lack of phototransduction leads to high levels of local oxygen concentrations that are only partially compensated for by the retinal vasculature [73,78]. This might then lead to the production of reactive oxygen species that have been shown to be damaging to cell survival. Other plausible explanations as to why the photoreceptors undergo apoptosis include metabolic stress created by the production of a large bolus of protein that is not properly trafficked in the cell body [42,73], or an inflammatory response of Muller glial cells undergoing reactive gliosis [79,80,81,82,83]. Finally, it is also possible that because the systemic problems resulting from *Mks3* mutation that arise may have some bearing on the degeneration of photoreceptors. We find the last to be an unlikely scenario, given that the mutation on a different genetic background leads to a less severe phenotype in kidney, but the photoreceptors still undergo a similar time course of degeneration (Gattone, unpublished data).

Just as interesting as the presence of photoreceptor degeneration is the apparent absence of degeneration in other cell types in the mutant retina. In addition to the inner and outer segment of WT retinae, MKS3 was also localized to Muller,

amacrine, and ganglion cells of the developing retina. While these cells express the MKS3, they appear not to undergo degeneration, at least during the period examined in the studies presented here. Barring the possibility that the cells degenerate later in development, perhaps the most logical reason these cells do not degenerate is that the cilia may be a vestigial apparatus in many cells [84]. Cilia are present in almost all cells, but they appear to have a function only in a subset of those cells [85]. Alternatively, cilia in these other cells may have an as yet undescribed function, but the cells are not as reliant upon this particular function for their survival [86]. Further study is needed to clarify the potential contribution(s) of MKS3 in other retinal cell types.

Ciliopathies and Retinal Degenerations

Many of the ciliopathies that affect the retinae also can cause pathological changes in other organs as well such as the kidney. Since Meckel Gruber Syndrome is probably the most severe of the renal ciliopathies, causing cysts to form in kidney, it would also likely cause a retinal phenotype as well. While six to ten different genes have been associated to MKS, it is unclear whether all will actually lead to a condition that resembles Leber's Congenital Amaurosis in humans. Leber's Amaurosis has been associated with a number of genes [87]. One of the genes that has previously been associated with Leber's amaurosis in both cats and humans, CEP290, can also cause Meckels Syndrome (aka MKS4) [88,89]. While truncation and gene deletion mutations of CEP290 can cause a full-blown Meckel Syndrome, other less severe mutations can cause a less severe phenotype that also includes Leber's Congenital Amaurosis. Interestingly, replacement of the N-terminal of CEP290 can restore the retina, at least in

zebrafish [90]. Thus far, MKS3 (or TMEM67) mutations have not been described as causing a Leber's Congenital Amaurosis in humans, only in the Wpk rat [58]. However, the disease in the Wpk rat involves many organs, including lethal renal cystic and brain pathology. A similar multiorgan phenotype has been identified with other types of congenital renal ciliopathies such as Bardt Beidl syndrome (BBS1, [91] : BBS4, [92,93]). However, Bardt Beidl Syndrome carriers of a BBS mutation also have a retinal phenotype [94].

After a number of animal model studies, gene therapy has now been used to ameliorate the visual deficit in RPE65 gene mutations in affected humans suggesting that this condition is amenable to treatment and correction [95,96]-[97,98]. However, in the retinal degeneration seen in the WPK rat herein, after the loss of rod cells, recovery would only be possible if treatment were started early. Since there were minimal changes prior to time outer segment normally develops, any such rescue in *Mks3*-induced disease would require the treatment of suckling rats. However, it is unclear how effective treatment would be in such a rapidly developing disease.

The Meckel Syndrome associated with an MKS3 mutation exhibits a severe retinal phenotype that resembles Leber's Congenital Amaurosis with the eventual loss of photoreceptor cells through apoptosis and an increase in glial scarring. While the remainder of the retinal cell types are largely preserved, any attempt at rescuing this rapidly developing degeneration of photoreceptors remains questionable. It is likely that other forms of Meckel Syndrome may also have a retinal phenotype; however, the severity of the pathology in other organs has limited the evaluation of the retina in affected humans.

Future Directions

There are several different directions to move to understand not only the affect of Meckel-Gruber syndrome on the retina, but also in trying to comprehend the mechanism of how the photoreceptors degenerate. First, the intraflagellar transport (IFT) process that the connecting cilium uses to transport important cargo for outer segment development should be better characterized. Meckelin has been localized to the basal body and axoneme of the primary cilia, however, which of the many proteins localized to these regions interact with meckelin is not clear. There are several known proteins that have been identified in participating in the IFT process [99]. Double-immunohistochemistry can be performed with meckelin and known IFT participating proteins to see which co-localize with meckelin. Next, co-immunoprecipitation using antibodies to those proteins that appear to co-localize with meckelin can be used to analyze the potential protein-protein interactions. The IFT motor proteins, kinesin and dynein, are a great place to start with because they are responsible for the transportation of cargo to the outer segment and back to the base of the cilium, respectfully. IFT20 is an IFT particle protein that previous studies have found to play a role in the transport of rhodopsin from the golgi complex to the base of the connecting cilium and has been found to localize to the inner segment, basal body and transition zone of primary cilia [100]. IFT88 and CEP290 are also localized to the basal body and axoneme of cilia and a loss of either leads to a lack of outer segment development [101,102]. Understanding what if any connection exists between these proteins and meckelin will be critical in our understanding of the mechanism of outer segment formation and maintenance.

In this study, we have been able to show through immunostaining and cell death assays that the Wpk mutant rat undergoes rapid photoreceptor degeneration between P10 and P21. One necessary aspect of the degeneration will be to confirm to when exactly the photoreceptor cells start to undergo apoptosis. This can be done by taking different aged rats between P10 and P21 and performing cell death assays to see the initial time point the photoreceptor cells start apoptosis. At P10, we found that all retinal cell types were present and similar in number when comparing the WT and mutant; however, it would be interesting to know if the photoreceptor cells are already programmed for cell death by P10. To perform this study, the use of annexin V could be used as an early cell death marker. Phosphatidylserine is a cell membrane phospholipid component and is confined to the inner leaflet of the plasma membrane. Once a cell initiates apoptosis, phosphatidylserine gets rapidly exposed on the cell's outer surface and can be detected through the use of an antibody specific for annexin V [103].

In addition to understanding the mechanisms of Meckel-Gruber syndrome within the retina, ways to recover or stop the degeneration of photoreceptor cells are also very important. One possible way to help the retina development a proper photoreceptor outer segment in the Wpk mutant rats is to introduce the absent meckelin protein through the uptake of nanoparticles. Nanoparticles can be made with proteins that are endocytosed by the developing photoreceptors, enabling replacement of missing mutated proteins. For this study, nanoparticles with meckelin could be made to target known receptors on the retina to see if the uptake of meckelin could regenerate photoreceptor outer segments or prevent the photoreceptors from undergoing apoptosis.

This study evaluated meckelin (MKS3 protein product) expression during normal postnatal retinal development and the consequences of mutant meckelin on photoreceptor development and survival in Wistar polycystic kidney disease Wpk/Wpk rat using immunohistochemistry, analysis of cell death and electron microscopy. Results showed that P21 mutant rats undergo rapid photoreceptor degeneration with no loss of other cell types. Meckelin is known to be localized to the connecting cilium and there are many known proteins have a role in the connecting cilium and IFT process. Hopefully with a better understanding of what meckelin is interacting with will help identify the source of the problem. Better understanding meckelin interactions would not only help with this current model, but with other known ciliopathies.

LIST OF REFERENCES

LIST OF REFERENCES

1. Chenoweth JG, McKay RD, Tesar PJ (2010) Epiblast stem cells contribute new insight into pluripotency and gastrulation. Dev Growth Differ 52: 293-301.
2. Greene ND, Copp AJ (2009) Development of the vertebrate central nervous system: formation of the neural tube. Prenat Diagn 29: 303-311.
3. Hyer J, Kuhlman J, Afif E, Mikawa T (2003) Optic cup morphogenesis requires pre-lens ectoderm but not lens differentiation. Dev Biol 259: 351-363.
4. Chow RL, Lang RA (2001) Early eye development in vertebrates. Annu Rev Cell Dev Biol 17: 255-296.
5. Kim JW, Lemke G (2006) Hedgehog-regulated localization of Vax2 controls eye development. Genes Dev 20: 2833-2847.
6. Bora N, Conway SJ, Liang H, Smith SB (1998) Transient overexpression of the Microphthalmia gene in the eyes of Microphthalmia vitiligo mutant mice. Dev Dyn 213: 283-292.
7. Rowan S, Chen CM, Young TL, Fisher DE, Cepko CL (2004) Transdifferentiation of the retina into pigmented cells in ocular retardation mice defines a new function of the homeodomain gene Chx10. Development 131: 5139-5152.
8. Liu IS, Chen JD, Ploder L, Vidgen D, van der Kooy D, et al. (1994) Developmental expression of a novel murine homeobox gene (Chx10): evidence for roles in determination of the neuroretina and inner nuclear layer. Neuron 13: 377-393.
9. Reh TA, Levine EM (1998) Multipotential stem cells and progenitors in the vertebrate retina. J Neurobiol 36: 206-220.
10. Rapaport DH, Wong LL, Wood ED, Yasumura D, LaVail MM (2004) Timing and topography of cell genesis in the rat retina. J Comp Neurol 474: 304-324.
11. La Vail MM, Rapaport DH, Rakic P (1991) Cytogenesis in the monkey retina. J Comp Neurol 309: 86-114.
12. Austin CP, Feldman DE, Ida JA, Jr., Cepko CL (1995) Vertebrate retinal ganglion cells are selected from competent progenitors by the action of Notch. Development 121: 3637-3650.
13. Ridge KD, Abdulaev NG, Sousa M, Palczewski K (2003) Phototransduction: crystal clear. Trends Biochem Sci 28: 479-487.
14. Roepman R, Wolfrum U (2007) Protein networks and complexes in photoreceptor cilia. Subcell Biochem 43: 209-235.
15. Kolb H (1995) Photoreceptors.

16. Moiseyev G, Chen Y, Takahashi Y, Wu BX, Ma JX (2005) RPE65 is the isomerohydrolase in the retinoid visual cycle. Proc Natl Acad Sci U S A 102: 12413-12418.
17. Chow RL, Volgyi B, Szilard RK, Ng D, McKerlie C, et al. (2004) Control of late off-center cone bipolar cell differentiation and visual signaling by the homeobox gene Vsx1. Proc Natl Acad Sci U S A 101: 1754-1759.
18. Feigenspan A, Weiler R (2004) Electrophysiological properties of mouse horizontal cell GABAA receptors. J Neurophysiol 92: 2789-2801.
19. Balboa RM, Grzywacz NM (2000) The minimal local-asperity hypothesis of early retinal lateral inhibition. Neural Comput 12: 1485-1517.
20. Watanabe M, Fukuda Y (1997) Proportions of ON-center versus OFF-center cells in retinal ganglion cells with regenerated axons of adult cats. Exp Neurol 143: 117-123.
21. Yang H, Downs JC, Sigal IA, Roberts MD, Thompson H, et al. (2009) Deformation of the normal monkey optic nerve head connective tissue after acute IOP elevation within 3-D histomorphometric reconstructions. Invest Ophthalmol Vis Sci 50: 5785-5799.
22. Rodieck RW (1979) Visual pathways. Annu Rev Neurosci 2: 193-225.
23. Hannula DE, Simons DJ, Cohen NJ (2005) Imaging implicit perception: promise and pitfalls. Nat Rev Neurosci 6: 247-255.
24. Nishida A, Furukawa A, Koike C, Tano Y, Aizawa S, et al. (2003) Otx2 homeobox gene controls retinal photoreceptor cell fate and pineal gland development. Nat Neurosci 6: 1255-1263.
25. Omori Y, Katoh K, Sato S, Muranishi Y, Chaya T, et al. (2011) Analysis of transcriptional regulatory pathways of photoreceptor genes by expression profiling of the otx2-deficient retina. PLoS One 6: e19685.
26. Freund CL, Gregory-Evans CY, Furukawa T, Papaioannou M, Looser J, et al. (1997) Cone-rod dystrophy due to mutations in a novel photoreceptor-specific homeobox gene (CRX) essential for maintenance of the photoreceptor. Cell 91: 543-553.
27. Furukawa T, Morrow EM, Cepko CL (1997) Crx, a novel otx-like homeobox gene, shows photoreceptor-specific expression and regulates photoreceptor differentiation. Cell 91: 531-541.
28. Mears AJ, Kondo M, Swain PK, Takada Y, Bush RA, et al. (2001) Nrl is required for rod photoreceptor development. Nat Genet 29: 447-452.
29. Hitchcock P, Kakuk-Atkins L (2004) The basic helix-loop-helix transcription factor neuroD is expressed in the rod lineage of the teleost retina. J Comp Neurol 477: 108-117.
30. Ochocinska MJ, Hitchcock PF (2009) NeuroD regulates proliferation of photoreceptor progenitors in the retina of the zebrafish. Mech Dev 126: 128-141.
31. Mustafi D, Engel AH, Palczewski K (2009) Structure of cone photoreceptors. Prog Retin Eye Res 28: 289-302.
32. Baker SA, Haeri M, Yoo P, Gospe SM, 3rd, Skiba NP, et al. (2008) The outer segment serves as a default destination for the trafficking of membrane proteins in photoreceptors. J Cell Biol 183: 485-498.

33. Sakurai K, Onishi A, Imai H, Chisaka O, Ueda Y, et al. (2007) Physiological properties of rod photoreceptor cells in green-sensitive cone pigment knock-in mice. J Gen Physiol 130: 21-40.
34. Adams NA, Awadein A, Toma HS (2007) The retinal ciliopathies. Ophthalmic Genet 28: 113-125.
35. Silverman MA, Leroux MR (2009) Intraflagellar transport and the generation of dynamic, structurally and functionally diverse cilia. Trends Cell Biol 19: 306-316.
36. Nilsson SE (1964) Receptor Cell Outer Segment Development and Ultrastructure of the Disk Membranes in the Retina of the Tadpole (Rana Pipiens). J Ultrastruct Res 11: 581-602.
37. Obata S, Usukura J (1992) Morphogenesis of the photoreceptor outer segment during postnatal development in the mouse (BALB/c) retina. Cell Tissue Res 269: 39-48.
38. Duldulao NA, Li J, Sun Z (2010) Cilia in cell signaling and human disorders. Protein Cell 1: 726-736.
39. Mitchell DR (2007) The evolution of eukaryotic cilia and flagella as motile and sensory organelles. Adv Exp Med Biol 607: 130-140.
40. Waters AM, Beales PL (2011) Ciliopathies: an expanding disease spectrum. Pediatr Nephrol 26: 1039-1056.
41. Badano JL, Mitsuma N, Beales PL, Katsanis N (2006) The ciliopathies: an emerging class of human genetic disorders. Annu Rev Genomics Hum Genet 7: 125-148.
42. Ramamurthy V, Cayouette M (2009) Development and disease of the photoreceptor cilium. Clin Genet 76: 137-145.
43. Mazor M, Alkrinawi S, Chalifa-Caspi V, Manor E, Sheffield VC, et al. (2011) Primary Ciliary Dyskinesia Caused by Homozygous Mutation in DNAL1, Encoding Dynein Light Chain 1. Am J Hum Genet 88: 599-607.
44. Sharma N, Berbari NF, Yoder BK (2008) Ciliary dysfunction in developmental abnormalities and diseases. Curr Top Dev Biol 85: 371-427.
45. Alexiev BA, Lin X, Sun CC, Brenner DS (2006) Meckel-Gruber syndrome: pathologic manifestations, minimal diagnostic criteria, and differential diagnosis. Arch Pathol Lab Med 130: 1236-1238.
46. Salonen R, Norio R (1984) The Meckel syndrome in Finland: epidemiologic and genetic aspects. Am J Med Genet 18: 691-698.
47. Mittermayer C, Lee A, Brugger PC (2004) Prenatal diagnosis of the Meckel-Gruber syndrome from 11th to 20th gestational week. Ultraschall Med 25: 275-279.
48. Kyttala M, Tallila J, Salonen R, Kopra O, Kohlschmidt N, et al. (2006) MKS1, encoding a component of the flagellar apparatus basal body proteome, is mutated in Meckel syndrome. Nat Genet 38: 155-157.
49. Roume J, Genin E, Cormier-Daire V, Ma HW, Mehaye B, et al. (1998) A gene for Meckel syndrome maps to chromosome 11q13. Am J Hum Genet 63: 1095-1101.
50. Valente EM, Logan CV, Mougou-Zerelli S, Lee JH, Silhavy JL, et al. (2010) Mutations in TMEM216 perturb ciliogenesis and cause Joubert, Meckel and related syndromes. Nat Genet 42: 619-625.
51. Morgan NV, Gissen P, Sharif SM, Baumber L, Sutherland J, et al. (2002) A novel locus for Meckel-Gruber syndrome, MKS3, maps to chromosome 8q24. Hum Genet 111: 456-461.

52. Baala L, Audollent S, Martinovic J, Ozilou C, Babron MC, et al. (2007) Pleiotropic effects of CEP290 (NPHP6) mutations extend to Meckel syndrome. Am J Hum Genet 81: 170-179.
53. Delous M, Baala L, Salomon R, Laclef C, Vierkotten J, et al. (2007) The ciliary gene RPGRIP1L is mutated in cerebello-oculo-renal syndrome (Joubert syndrome type B) and Meckel syndrome. Nat Genet 39: 875-881.
54. Tallila J, Jakkula E, Peltonen L, Salonen R, Kestila M (2008) Identification of CC2D2A as a Meckel syndrome gene adds an important piece to the ciliopathy puzzle. Am J Hum Genet 82: 1361-1367.
55. Bergmann C, Fliegauf M, Bruchle NO, Frank V, Olbrich H, et al. (2008) Loss of nephrocystin-3 function can cause embryonic lethality, Meckel-Gruber-like syndrome, situs inversus, and renal-hepatic-pancreatic dysplasia. Am J Hum Genet 82: 959-970.
56. Karmous-Benailly H, Martinovic J, Gubler MC, Sirot Y, Clech L, et al. (2005) Antenatal presentation of Bardet-Biedl syndrome may mimic Meckel syndrome. Am J Hum Genet 76: 493-504.
57. Smith UM, Consugar M, Tee LJ, McKee BM, Maina EN, et al. (2006) The transmembrane protein meckelin (MKS3) is mutated in Meckel-Gruber syndrome and the wpk rat. Nat Genet 38: 191-196.
58. Tammachote R, Hommerding CJ, Sinders RM, Miller CA, Czarnecki PG, et al. (2009) Ciliary and centrosomal defects associated with mutation and depletion of the Meckel syndrome genes MKS1 and MKS3. Hum Mol Genet 18: 3311-3323.
59. Dawe HR, Smith UM, Cullinane AR, Gerrelli D, Cox P, et al. (2007) The Meckel-Gruber Syndrome proteins MKS1 and meckelin interact and are required for primary cilium formation. Hum Mol Genet 16: 173-186.
60. Gattone VH, 2nd, Tourkow BA, Trambaugh CM, Yu AC, Whelan S, et al. (2004) Development of multiorgan pathology in the wpk rat model of polycystic kidney disease. Anat Rec A Discov Mol Cell Evol Biol 277: 384-395.
61. Wilson JM, Sato K, Chernoff EA, Belecky-Adams TL (2007) Expression patterns of chick Musashi-1 in the developing nervous system. Gene Expr Patterns 7: 817-825.
62. Williams CL, Masyukova SV, Yoder BK (2010) Normal Ciliogenesis Requires Synergy between the Cystic Kidney Disease Genes MKS-3 and NPHP-4. Journal of the American Society of Nephrology 21: 782-793.
63. Pagh-Roehl K, Wang E, Burnside B (1991) Posttranslational modifications of tubulin in teleost photoreceptor cytoskeletons. Cell Mol Neurobiol 11: 593-610.
64. Nauta J, Goedbloed MA, Herck HV, Hesselink DA, Visser P, et al. (2000) New rat model that phenotypically resembles autosomal recessive polycystic kidney disease. J Am Soc Nephrol 11: 2272-2284.
65. Gattone VH, 2nd, Wang X, Harris PC, Torres VE (2003) Inhibition of renal cystic disease development and progression by a vasopressin V2 receptor antagonist. Nat Med 9: 1323-1326.
66. De Robertis E (1960) Some observations on the ultrastructure and morphogenesis of photoreceptors. J Gen Physiol 43(6)Suppl: 1-13.

67. Olney JW (1968) An electron microscopic study of synapse formation, receptor outer segment development, and other aspects of developing mouse retina. Invest Ophthalmol 7: 250-268.
68. Steinberg RH, Fisher SK, Anderson DH (1980) Disc morphogenesis in vertebrate photoreceptors. J Comp Neurol 190: 501-508.
69. Chang GQ, Hao Y, Wong F (1993) Apoptosis: final common pathway of photoreceptor death in rd, rds, and rhodopsin mutant mice. Neuron 11: 595-605.
70. Papermaster DS (2002) The birth and death of photoreceptors: the Friedenwald Lecture. Invest Ophthalmol Vis Sci 43: 1300-1309.
71. Portera-Cailliau C, Sung CH, Nathans J, Adler R (1994) Apoptotic photoreceptor cell death in mouse models of retinitis pigmentosa. Proc Natl Acad Sci U S A 91: 974-978.
72. Rattner A, Nathans J (2006) An evolutionary perspective on the photoreceptor damage response. Am J Ophthalmol 141: 558-562.
73. Bramall AN, Wright AF, Jacobson SG, McInnes RR (2010) The genomic, biochemical, and cellular responses of the retina in inherited photoreceptor degenerations and prospects for the treatment of these disorders. Annu Rev Neurosci 33: 441-472.
74. Colicos MA, Dash PK (1996) Apoptotic morphology of dentate gyrus granule cells following experimental cortical impact injury in rats: possible role in spatial memory deficits. Brain Res 739: 120-131.
75. Grasl-Kraupp B, Ruttkay-Nedecky B, Koudelka H, Bukowska K, Bursch W, et al. (1995) In situ detection of fragmented DNA (TUNEL assay) fails to discriminate among apoptosis, necrosis, and autolytic cell death: a cautionary note. Hepatology 21: 1465-1468.
76. Doonan F, Donovan M, Cotter TG (2005) Activation of multiple pathways during photoreceptor apoptosis in the rd mouse. Invest Ophthalmol Vis Sci 46: 3530-3538.
77. Sancho-Pelluz J, Arango-Gonzalez B, Kustermann S, Romero FJ, van Veen T, et al. (2008) Photoreceptor cell death mechanisms in inherited retinal degeneration. Mol Neurobiol 38: 253-269.
78. Noell WK (1953) Experimentally induced toxic effects on structure and function of visual cells and pigment epithelium. Am J Ophthalmol 36: 103-116.
79. Hackam AS, Strom R, Liu D, Qian J, Wang C, et al. (2004) Identification of gene expression changes associated with the progression of retinal degeneration in the rd1 mouse. Invest Ophthalmol Vis Sci 45: 2929-2942.
80. Kamphuis W, Dijk F, van Soest S, Bergen AA (2007) Global gene expression profiling of ischemic preconditioning in the rat retina. Mol Vis 13: 1020-1030.
81. Nakazawa T, Takeda M, Lewis GP, Cho KS, Jiao J, et al. (2007) Attenuated glial reactions and photoreceptor degeneration after retinal detachment in mice deficient in glial fibrillary acidic protein and vimentin. Invest Ophthalmol Vis Sci 48: 2760-2768.
82. Rattner A, Nathans J (2005) The genomic response to retinal disease and injury: evidence for endothelin signaling from photoreceptors to glia. J Neurosci 25: 4540-4549.

83. Verardo MR, Lewis GP, Takeda M, Linberg KA, Byun J, et al. (2008) Abnormal reactivity of muller cells after retinal detachment in mice deficient in GFAP and vimentin. Invest Ophthalmol Vis Sci 49: 3659-3665.
84. Wheatley DN (1995) Primary cilia in normal and pathological tissues. Pathobiology 63: 222-238.
85. Wheatley DN, Wang AM, Strugnell GE (1996) Expression of primary cilia in mammalian cells. Cell Biol Int 20: 73-81.
86. Poole CA, Jensen CG, Snyder JA, Gray CG, Hermanutz VL, et al. (1997) Confocal analysis of primary cilia structure and colocalization with the Golgi apparatus in chondrocytes and aortic smooth muscle cells. Cell Biol Int 21: 483-494.
87. Chung DC, Traboulsi EI (2009) Leber congenital amaurosis: clinical correlations with genotypes, gene therapy trials update, and future directions. J AAPOS 13: 587-592.
88. Menotti-Raymond M, David VA, Schaffer AA, Stephens R, Wells D, et al. (2007) Mutation in CEP290 discovered for cat model of human retinal degeneration. J Hered 98: 211-220.
89. Simonelli F, Ziviello C, Testa F, Rossi S, Fazzi E, et al. (2007) Clinical and molecular genetics of Leber's congenital amaurosis: a multicenter study of Italian patients. Invest Ophthalmol Vis Sci 48: 4284-4290.
90. Baye LM, Patrinostro X, Swaminathan S, Beck JS, Zhang Y, et al. (2011) The N-terminal region of centrosomal protein 290 (CEP290) restores vision in a zebrafish model of human blindness. Hum Mol Genet.
91. Azari AA, Aleman TS, Cideciyan AV, Schwartz SB, Windsor EA, et al. (2006) Retinal disease expression in Bardet-Biedl syndrome-1 (BBS1) is a spectrum from maculopathy to retina-wide degeneration. Invest Ophthalmol Vis Sci 47: 5004-5010.
92. Abd-El-Barr MM, Sykoudis K, Andrabi S, Eichers ER, Pennesi ME, et al. (2007) Impaired photoreceptor protein transport and synaptic transmission in a mouse model of Bardet-Biedl syndrome. Vision Res 47: 3394-3407.
93. Swiderski RE, Nishimura DY, Mullins RF, Olvera MA, Ross JL, et al. (2007) Gene expression analysis of photoreceptor cell loss in bbs4-knockout mice reveals an early stress gene response and photoreceptor cell damage. Invest Ophthalmol Vis Sci 48: 3329-3340.
94. Kim LS, Fishman GA, Seiple WH, Szlyk JP, Stone EM (2007) Retinal dysfunction in carriers of bardet-biedl syndrome. Ophthalmic Genet 28: 163-168.
95. Lai CM, Yu MJ, Brankov M, Barnett NL, Zhou X, et al. (2004) Recombinant adeno-associated virus type 2-mediated gene delivery into the Rpe65-/- knockout mouse eye results in limited rescue. Genet Vaccines Ther 2: 3.
96. Pang J, Boye SE, Lei B, Boye SL, Everhart D, et al. (2010) Self-complementary AAV-mediated gene therapy restores cone function and prevents cone degeneration in two models of Rpe65 deficiency. Gene Ther 17: 815-826.
97. Bainbridge JW, Smith AJ, Barker SS, Robbie S, Henderson R, et al. (2008) Effect of gene therapy on visual function in Leber's congenital amaurosis. N Engl J Med 358: 2231-2239.

98. Simonelli F, Maguire AM, Testa F, Pierce EA, Mingozzi F, et al. (2010) Gene therapy for Leber's congenital amaurosis is safe and effective through 1.5 years after vector administration. Mol Ther 18: 643-650.
99. Cao Y, Park A, Sun Z (2010) Intraflagellar transport proteins are essential for cilia formation and for planar cell polarity. J Am Soc Nephrol 21: 1326-1333.
100. Keady BT, Le YZ, Pazour GJ (2011) IFT20 is required for opsin trafficking and photoreceptor outer segment development. Mol Biol Cell 22: 921-930.
101. Chang B, Khanna H, Hawes N, Jimeno D, He S, et al. (2006) In-frame deletion in a novel centrosomal/ciliary protein CEP290/NPHP6 perturbs its interaction with RPGR and results in early-onset retinal degeneration in the rd16 mouse. Hum Mol Genet 15: 1847-1857.
102. Robert A, Margall-Ducos G, Guidotti JE, Bregerie O, Celati C, et al. (2007) The intraflagellar transport component IFT88/polaris is a centrosomal protein regulating G1-S transition in non-ciliated cells. J Cell Sci 120: 628-637.
103. Blankenberg FG, Katsikis PD, Tait JF, Davis RE, Naumovski L, et al. (1999) Imaging of apoptosis (programmed cell death) with 99mTc annexin V. J Nucl Med 40: 184-191.
104. Lamb TD, Collin SP, Pugh EN, Jr. (2007) Evolution of the vertebrate eye: opsins, photoreceptors, retina and eye cup. Nat Rev Neurosci 8: 960-976.
105. Livesey FJ, Cepko CL (2001) Vertebrate neural cell-fate determination: lessons from the retina. Nat Rev Neurosci 2: 109-118.
106. Lamb TD (2009) Evolution of vertebrate retinal photoreception. Philos Trans R Soc Lond B Biol Sci 364: 2911-2924.
107. Schmitt A, Wolfrum U (2001) Identification of novel molecular components of the photoreceptor connecting cilium by immunoscreens. Exp Eye Res 73: 837-849.
108. Fetter RD, Corless JM (1987) Morphological components associated with frog cone outer segment disc margins. Invest Ophthalmol Vis Sci 28: 646-657.

TABLES

Table 1.1 Ciliopathies with Overlapping Phenotypes. Table includes well know ciliopathies and the phenotypes associated with each syndrome. This table shows the overlap in phenotypes between the diseases.

Phenotype	**Ciliopathies**					
	LCA	SLS	NPHP	MKS	BBS	JBTS
Cerebellar			√		√	√
Hypoplasia						
Encephalocele				√		
Hepatic disease		√	√	√	√	√
Renal disease		√	√	√	√	√
Mental Retardation	√		√		√	√
Obesity					√	√
Polydactyly				√	√	√
Retinopathy	√	√	√	√	√	√
Situs inversus		√	√	√	√	√
Skeletal dysplasia				√		
Cleft palate				√		

LCA – Leber's congenital amaurosis; SLS – Senior-Loken syndrome; NPHP – nephronophthisis; MKS – Meckel-Gruber syndrome; BBS – Bardet-Biedl syndrome; JBS – Joubert syndrome; [37]

Table 2.1 Primary Antibodies Used for Immunohistochemistry.

Antibodies			
Antibody Name	Supplier	Catalog Number	Dilution
Tubulin	Sigma-Aldrich (St. Louis, MO)	T 6793	1:4,000
Calbindin-D-28k	Sigma-Aldrich (St. Louis, MO)	CB-955	1:200
Sox2	Santa Cruz (Santa Cruz, CA)	sc-17320	1:250
Opsin Blue	Millipore (Temecula, CA)	AB5407	1:200
Opsin Red/Green	Millipore (Temecula, CA)	AB5405	1:200
OPN1MW/MW2/LW	Santa Cruz (Santa Cruz, CA)	sc-22117	1:250
Rhodopsin	Millipore (Temecula, CA)	MAB5356	1:250
Meckelin	Novus (Littleton, CO)	NBP1-06590	1:200
Parvalbumin (Rabbit polyclonal)	Abcam (Cambridge, MA)	ab11427	1:2,000
Parvalbumin (Mouse monoclonal)	Sigma-Aldrich (St. Louis, MO)	P3088	1:2,000
GFAP	Dako (Carpinteria, CA)	Z0334	1:500
Brn3a	Millipore (Temecula, CA)	MAB1585	1:100
Chx10	Exalpha (Shirley, MA)	X1180P	1:500
Caspase 3	Cell Signaling (Danvers, MA)	Asp175	1:12,000

FIGURES

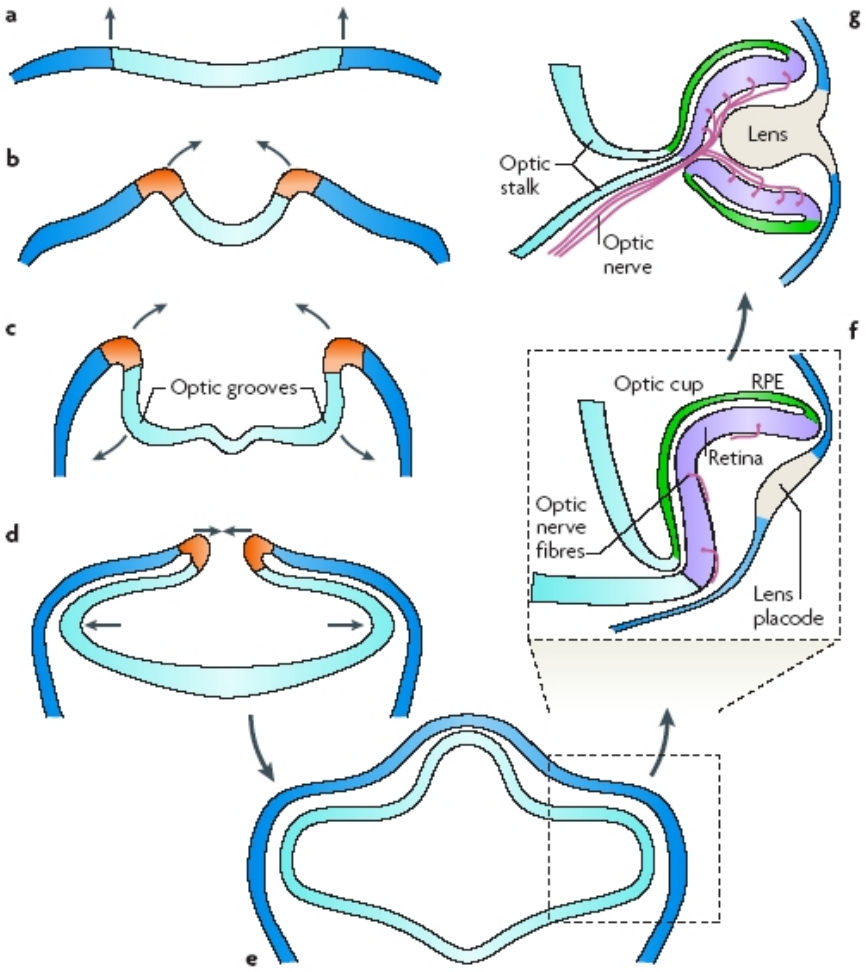

Figure 1.1 Eye Formation During Embryonic Development. The neural plate, in light blue (a), is induced from ectoderm by underlying pre-chordal mesoderm. At the beginning of eye formation, the neural plate folds inward to form a neural tube (a-d). As this is occurring, two small pits appear at either side of the neural plate, known as optic grooves, which herald the first visible sign of eye development. As the neural plate is undergoing closure, the optic grooves evaginate and enlarge to form the optic vesicles (e). The optic vesicles communicate with the surface ectoderm to form the lens placode (f). Simultaneously, the optic vesicle and lens placode invaginate to form the optic cup and lens vesicle, respectively (g). The inner part of the optic cup will become the multi-layered neural retina and the outer part will become the single layered retinal pigmented epithelium [104].

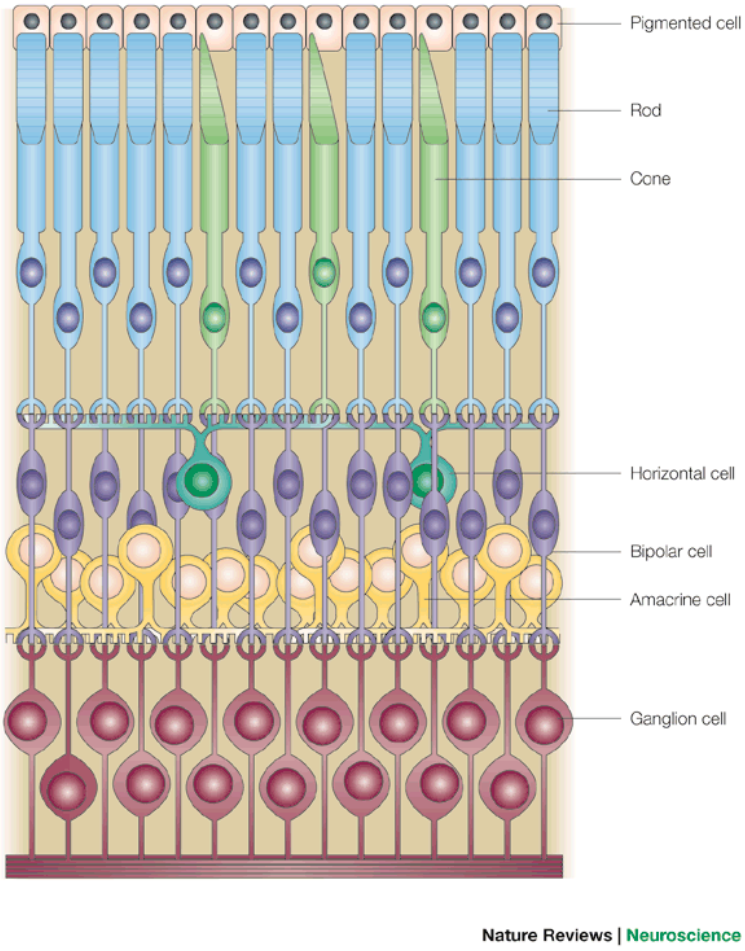

Figure 1.2 **The Vertebrate Retina.** The vertebrate retina is a multi-layered tissue consisting of cell bodies in the retinal pigmented epithelium, outer, inner, and ganglion cell layers. The outer nuclear layer (ONL) contains 2 type of photoreceptors; rods and cones. The inner nuclear layer contains horizontal, bipolar, Muller glia and amacrine cells. The ganglion cell layer contains ganglion cells and a subset of "displaced" amacrine and cells. Light enters at the ganglion cell layer and make its way to the outer segments of the photoreceptors. Photoreceptors then transform the light into biological signals through a process called phototransduction [105].

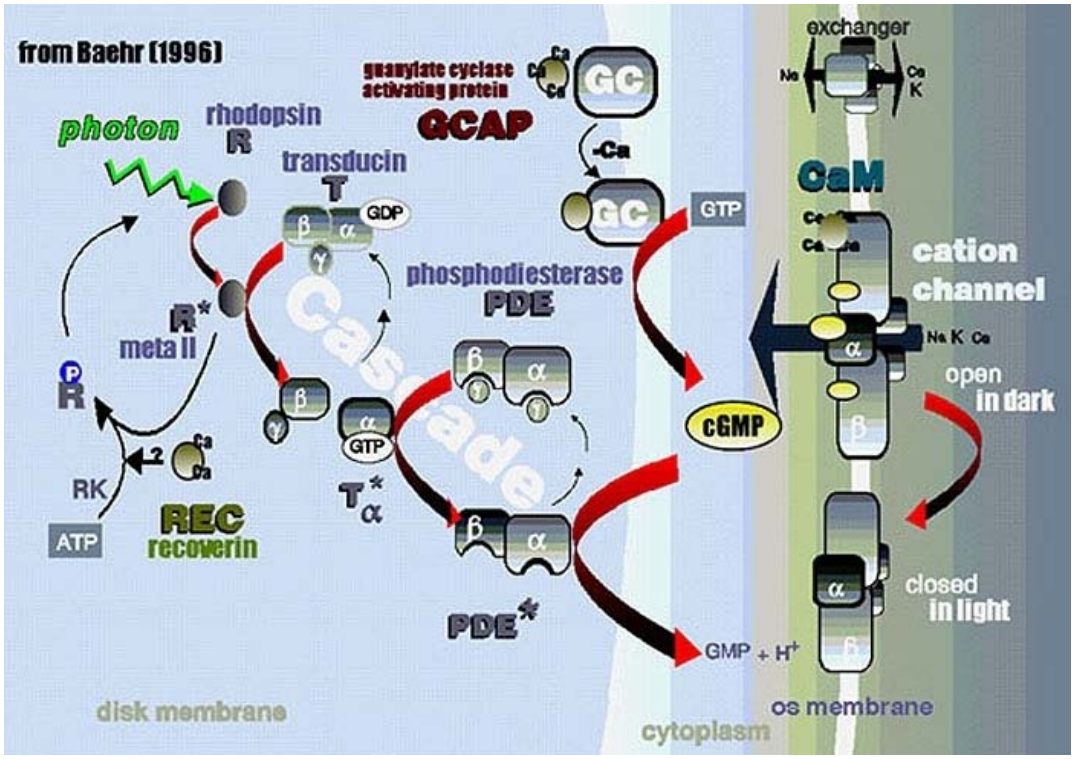

Figure 1.3 Phototransduction in Photoreceptor Outer Segment. The main function of the retina is to turn light into a biological signal through phototransduction. In the presence of light, visual pigment in stacked discs of the outer segment will absorb light. The visual pigment is comprised of the vitamin A derivative, retinal, and a protein known as an opsin. When bound to the opsin, retinal is in the conformation referred to as N-cis retinal. Once light is absorbed by the N-cis retinal, it causes a conformational change that leads to the formation of the all-trans isomer of retinal. The opsin/all-trans retinal then activates the trimeric G-protein transducin, causing the α subunit of transducin to exchange GDP for GTP. This GTP complex will activate phosphodiesterase and will lead to the breakdown of cGMP to 5'-GMP. This breakdown will lower cGMP concentration and close the cation channels. Closure of the cation channels will cause the cell to hyperpolarize. This will result in a decrease the amount of glutamate released from the synaptic region of photoreceptors [14].

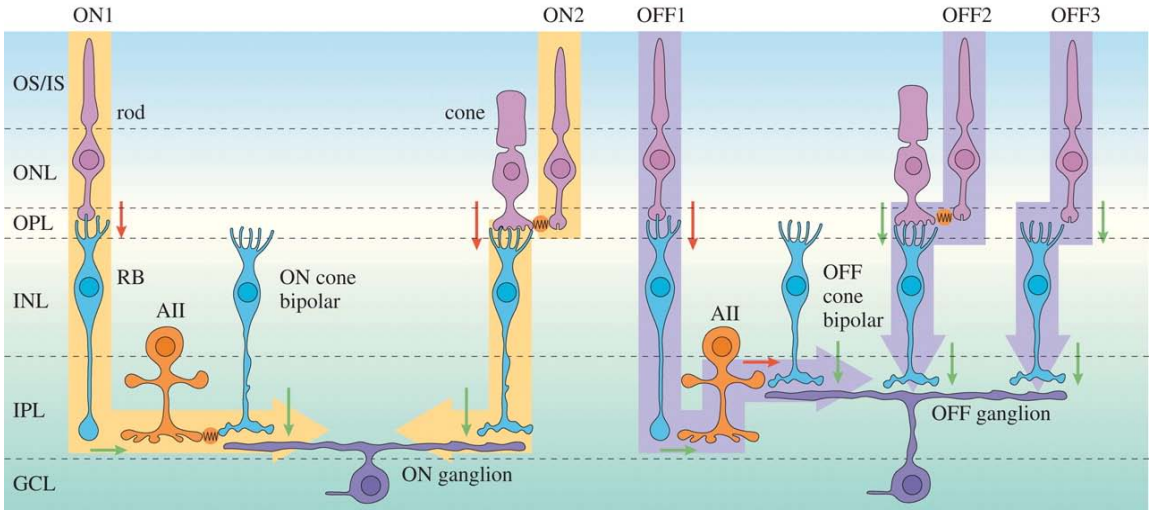

Figure 1.4 **Light Pathway in the Retina.** Photoreceptors make synapses with both bipolar and horizontal cells in the outer plexiform later of the retina. Photoreceptors have synapses with bipolar cells that are on- or off-center. An on-center bipolar cell is stimulated when the center of its receptive field is exposed to light and inhibited when light hits the surrounding area. The off-center bipolar cells have an opposite reaction of being inhibited with direct light to the center and excited when light is exposed in the surrounding area. Ganglion cells also have on- and off-center cells that function in the same way as bipolar cells. Ganglion cells project their axons to the optic nerve head, where they bundle axons together to form the optic nerve [106].

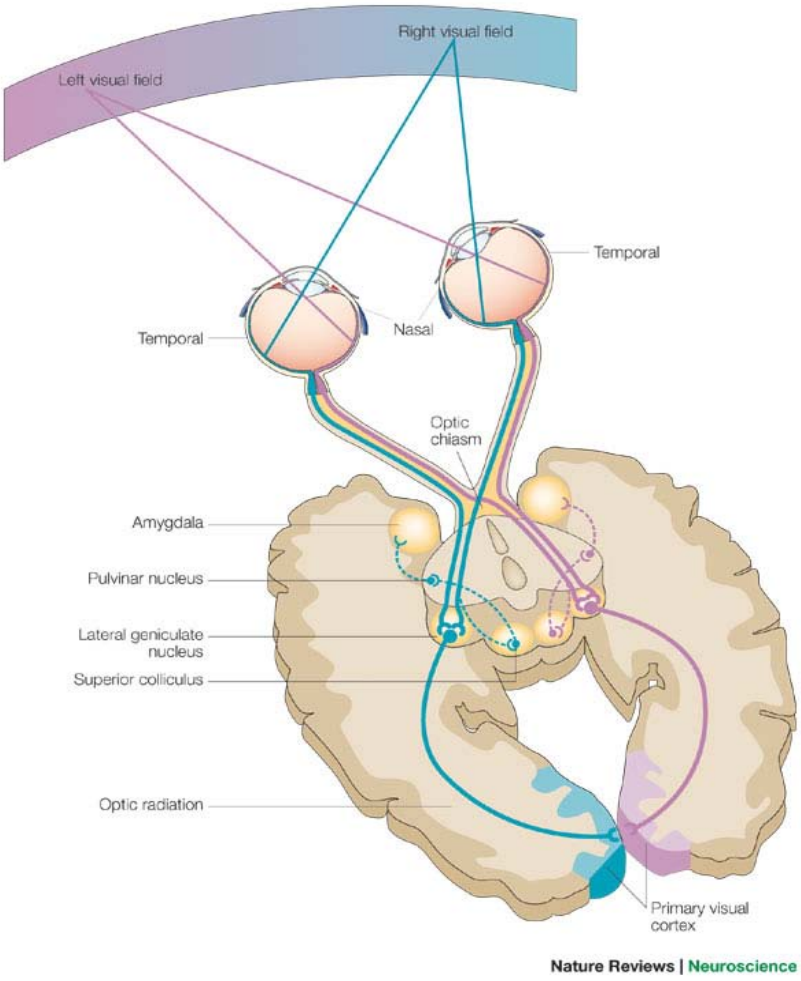

Figure 1.5 The Pathway of the Visual System. As the light signal that starts at the photoreceptors is transferred to the ganglion cells, the ganglion cells then project their axons to the optic nerve head, the axons are bundled together to form the optic nerve. Ganglion cell axons project toward the midline of the CNS, at a region known as the optic chiasm. In humans, information from the temporal retina remains ipsilateral (e.g. information from right temporal retina goes to right hemisphere of brain). The opposite happens with the nasal retina, as the information received will project contralaterally (e.g. information from the right nasal side will cross over and go to the left hemisphere of the brain). From the optic chiasm, axons project to the pretectum, superior colliculus or lateral geniculate nucleus (LGN). The cells of the LGN then project to the visual cortex, where information transduced in the retina is perceived [23].

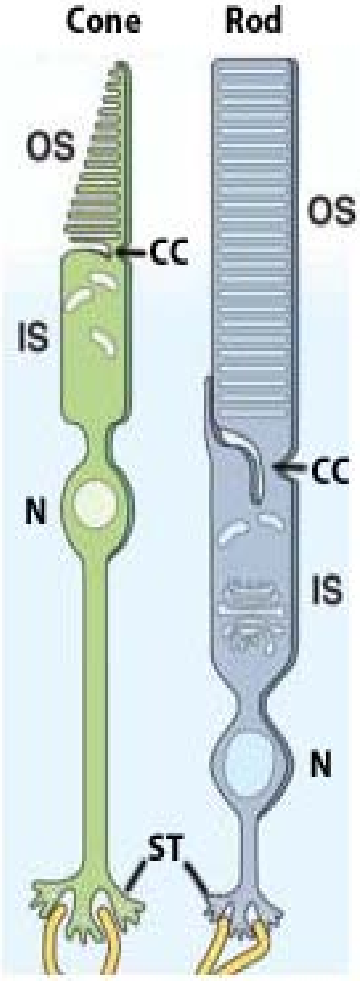

Figure 1.6 Structures of Photoreceptor Rods and Cones. Photoreceptor rods and cones have many similarities. Rods and cones have synaptic terminals (ST) containing the neurotransmitter glutamate that is released at the synaptic ending to interact with bipolar and horizontal cells. They have an inner segment (IS) where the visual pigment is made. They each have a cell nucleus (N) and a connecting cilium (CC) that is used to transport important cargo for outer segment formation and function. Lastly, rods and cones have an outer segment (OS) full of discs that contain visual pigment for phototransduction. In rods, the disks pinch off from the plasma membrane, while the cone cells have discs that are continuous with the plasma membrane. Photoreceptor cone cells are smaller and fewer in number when compared to photoreceptor rod cells [31].

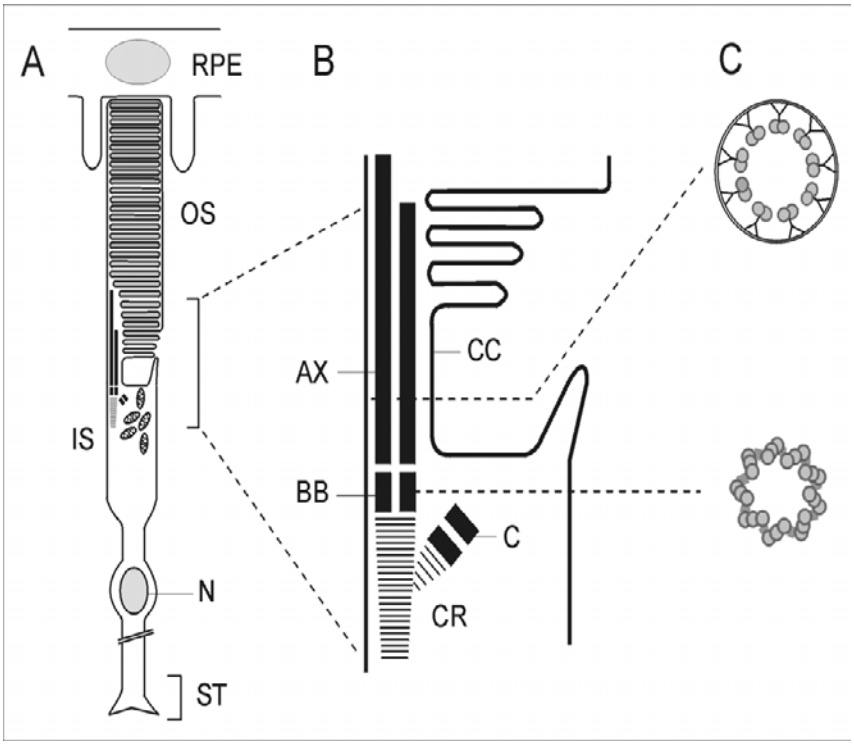

Figure 1.7 Photoreceptor Connecting Cilium. A) Photoreceptors can be divided into outer segments (OS), inner segment (IS), nucleus (N), and synaptic terminal (ST). B) Photoreceptor has a connecting cilium (CC) that connects the inner segment to the outer. The CC is a primary non-motile cilia that has nine-microtubule doublets with no center pair. The photoreceptor CC plays an essential role in the development/maintenance of the outer segment and transport important cargo, like visual pigment, necessary for phototransduction. C) The cilia is composed of nine microtubule-doublets without a center pair, making it a non-motile and function as a sensory organelle [107]. (AX- axoneme; BB- basal body; CR- ciliary rootlet; C- centriole)

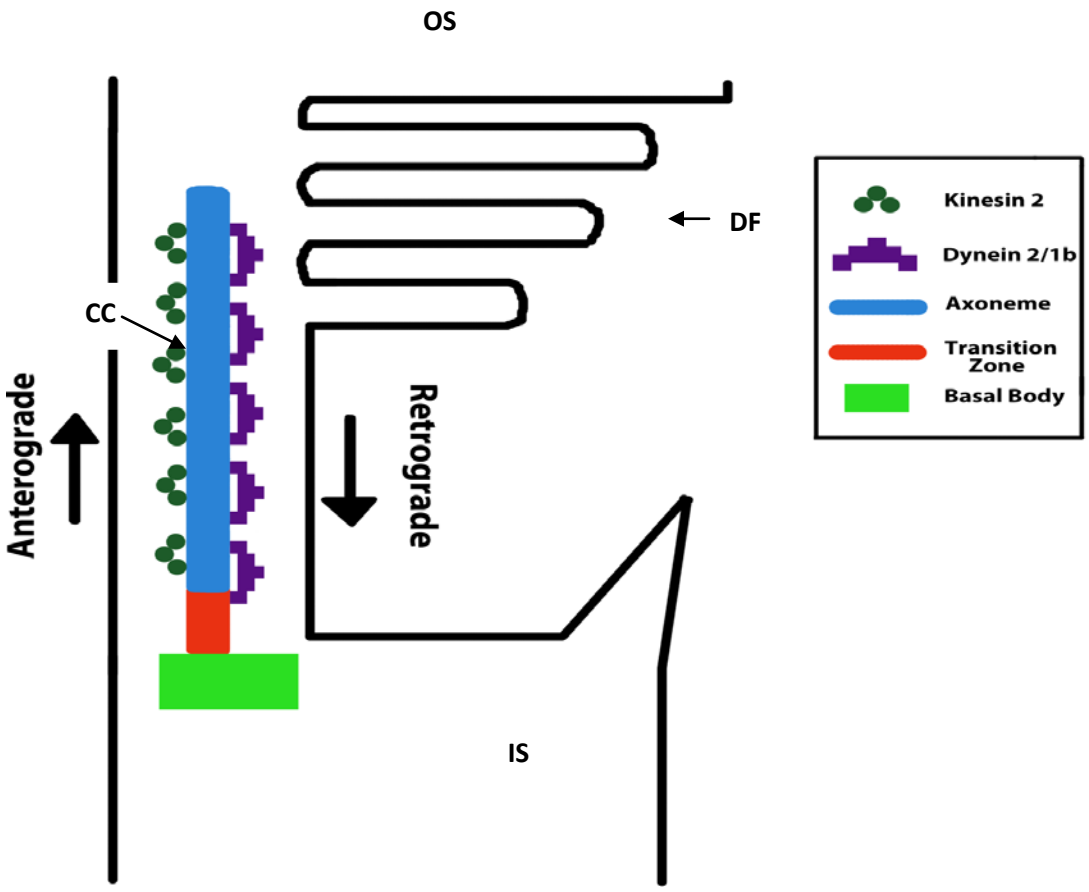

Figure 1.8 Intraflagellar Transport in Photoreceptor Connecting Cilium. The main function of the photoreceptor connecting cilium is to transport cargo from the inner segment (IS) to the outer segment (OS). To accomplish this function, the connecting cilium (CC) uses a process called intraflagellar transport. Cargo at the base of the CC will use the motor protein kinesin to be transported from the inner segment to the outer segment. This is referred to as anterograde transport. Cargo being taken back to the inner segment from the outer segment will use the motor protein called dynein. This is referred to as retrograde transport. The function the CC uses IFT for is disc formation (DF) [42].

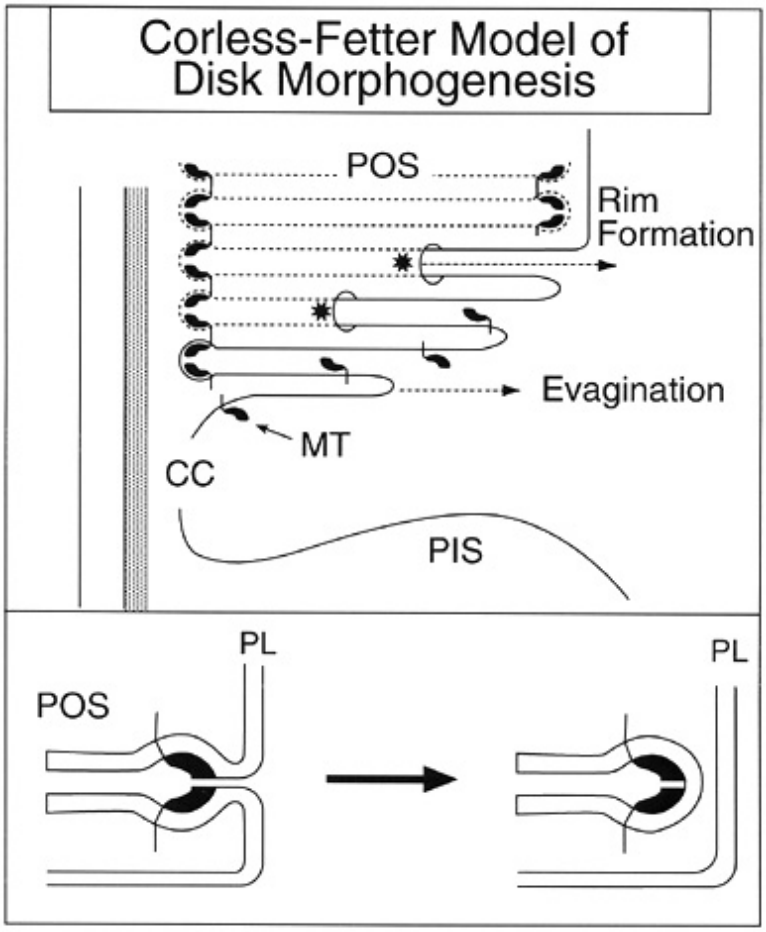

Figure 1.9 Outer Segment Formation by Invagination of Plasma Membrane. The Corless-Fetter model photoreceptor outer segment (POS) disc formation proposes that discs are formed through invagination of the plasma membrane (PL). After a cell has started to differentiate as a photoreceptor, a primary cilia will form and elongate on the apical end of the cell. As the connecting cilium (CC) extends out of the photoreceptor inner segment (PIS), the plasma membrane forms a balloon-like structure around the connecting cilium. Next, the growing plasma membrane invaginates to form discs. The extracellular margin templates (MT) become aligned and assemble to form terminal loop complexes, which are thought to represent the primary morphogen of the disc rims. In the bottom picture, disc rim formation is completed and pinches off from the plasma membrane [108].

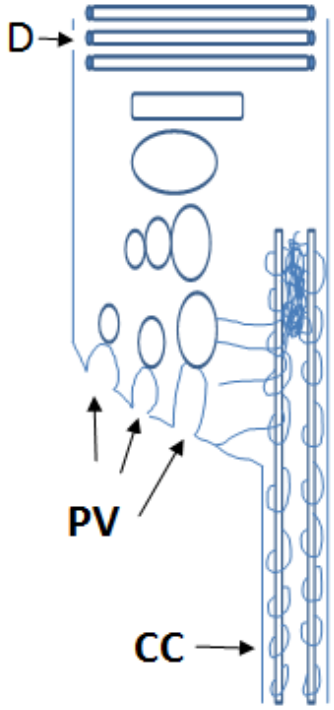

Figure 1.10 Outer Segment Formation by Pinocytosis. Another proposed theory of photoreceptor outer segments disc (D) formation is the pinocytic model. As the photoreceptor begins to differentiate, a primary cilia (CC) forms and elongates on the apical end of the cell. As the connecting cilium extends, the plasma membrane forms a balloon-like structure around the connecting cilium. At the base of the outer segment, pinocytic vesicles (PV) are fused, compressed by unknown mechanisms and then stacked together [37].

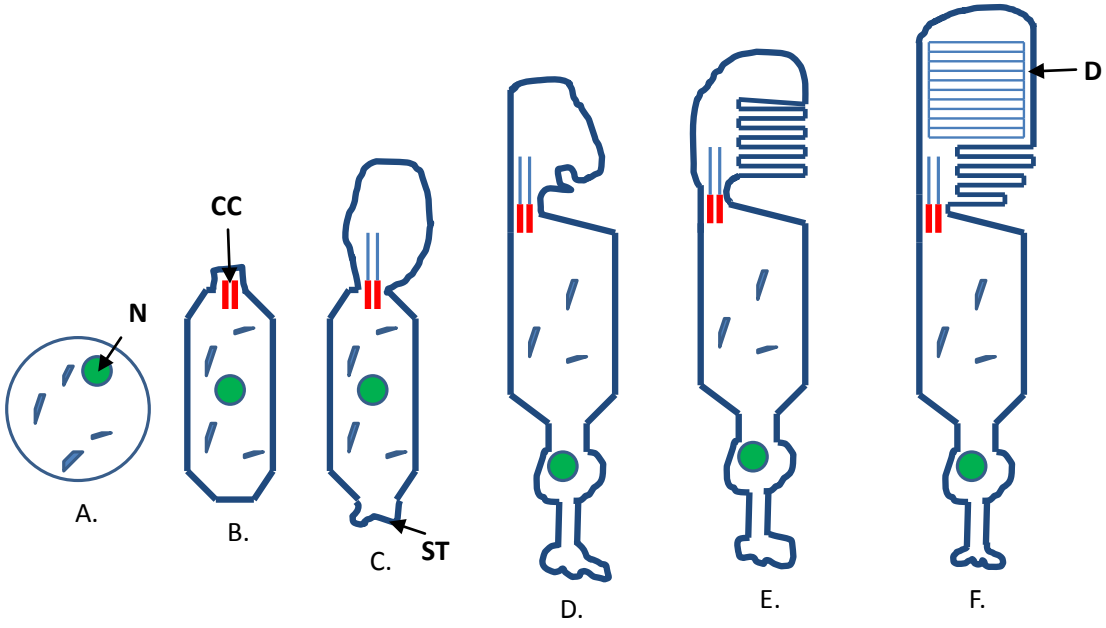

Figure 1.11 Development of Rod Photoreceptor. A) Photoreceptors develop from a pool of dividing progenitor cells in the vertebrate retina. Nuclear region (N) is shown in green. B) The connecting cilia (CC) extends from the apical side of the photoreceptor and is anchored by the basal body. C) The plasma membrane creates a balloon-like structure that surrounds the connecting cilium. D) The plasma membrane grows and forms an invagination. E-F) Invaginations continue and form disc like structures. The discs (D) are then pinched off, compressed, and stacked [35]. (ST-synaptic terminal)

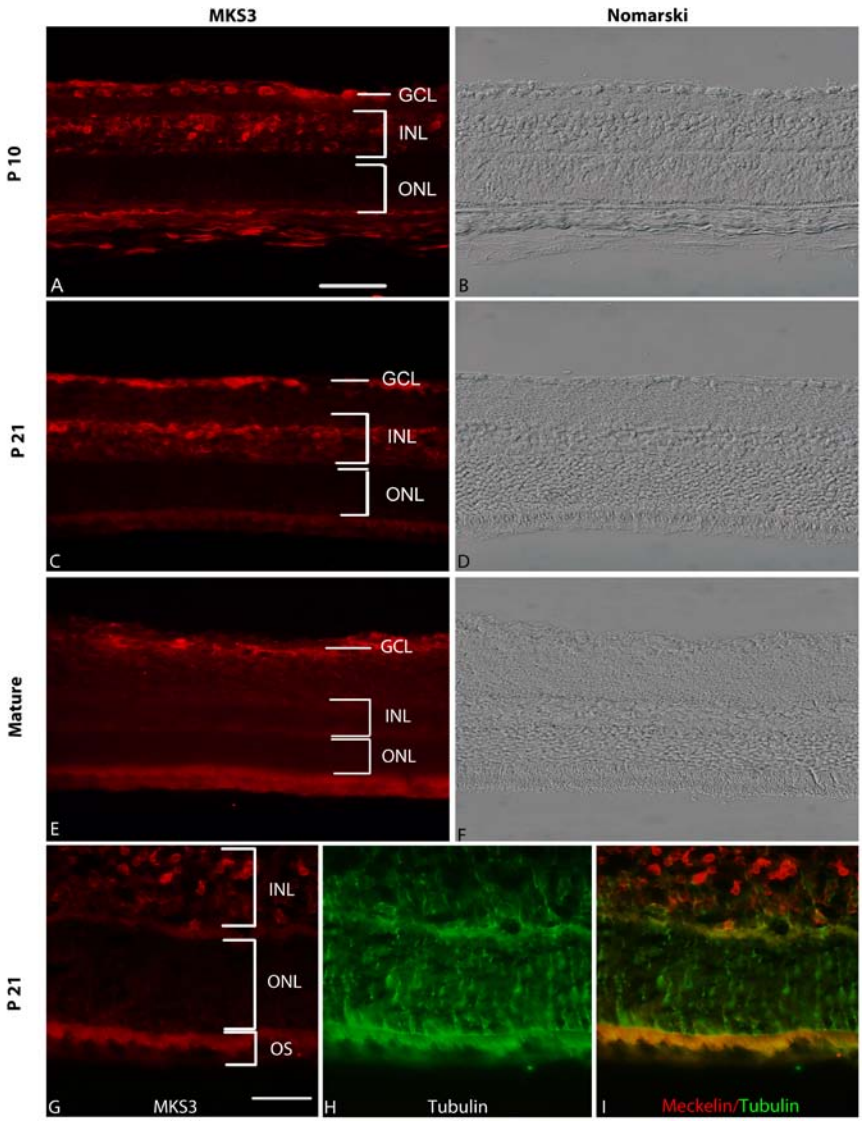

Figure 3.1 Meckelin 3 in the Developing Rat Retina. Immunohistological staining of MKS3 was observed in the outer, inner, and ganglion cell layers of retinae obtained from WT P10 (A), P21 (C), and mature (E) rats. Nomarski optics of the same sections are shown in B, D and F. Tissue sections were double labeled with MKS3 (G) and tubulin (H) to highlight the axoneme of the outer segment. An overlay of MKS3- and tubulin-label showed clear co-localization of the two proteins at the axoneme (I). GCL, ganglion cell layer; INL, inner nuclear layer; ONL, outer nuclear layer; OS, outer segment. Scale bar: (A) 50µm; (G) 50µm.

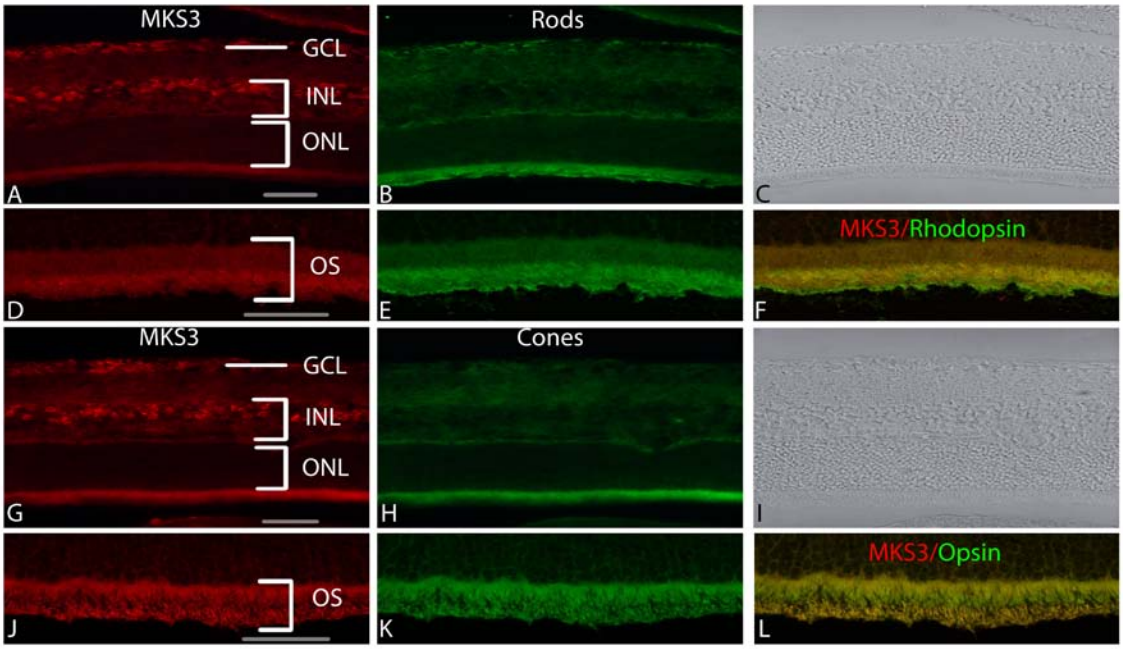

Figure 3.2 MKS3 is Found in Rods and Cones. Double-label immunohistochemistry was performed on sections through P21 WT retina using an antibody specific for MKS3 (A, D, G and J) and rhodopsin (B, E) or long/medium wavelength opsin (H, K). Images were then merged into a single image (F, L) to show the co-expression of MKS3 and photoreceptors in the outer segment. Nomarski optics is shown for each section (C, I). GCL, ganglion cell layer; INL, inner nuclear layer; ONL, outer nuclear layer; OS, outer segment. Scale bar: (A) 50µm.

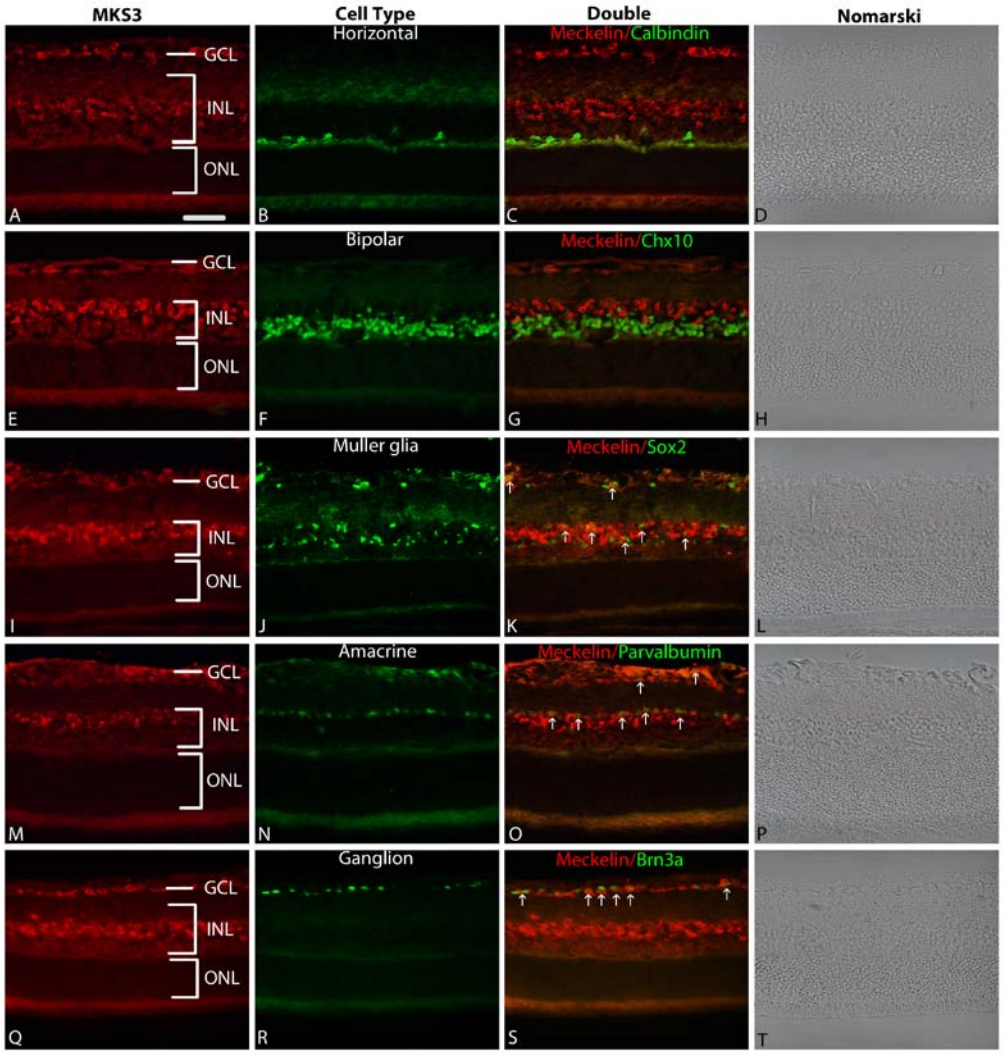

Figure 3.3 MKS3 is Widely Expressed in the Rat Retina. Double-label immunohistochemistry was performed in P21 retina with MKS3 (A, E, I, M and Q) and calbindin (horizontal cells) (B), Chx10 (bipolar cells) (F), Sox2 (Muller glia) (J), parvalbumin (amacrine cells) (N) or Brn3a (ganglion cells) (R). Co-expression of meckelin with these markers can be seen in C, G, K, O, and S. MKS3 appeared to be co-expressed in cells that were positive for Sox2, parvalbumin and Brn3a (arrows indicate co-expression). No co-expression appeared to be present in cells positive for calbindin and Chx10. Nomarski optics is shown for each section in D, H, L, P and T. GCL, ganglion cell layer; INL, inner nuclear layer; ONL, outer nuclear layer. Scale bar: (A) 50µm.

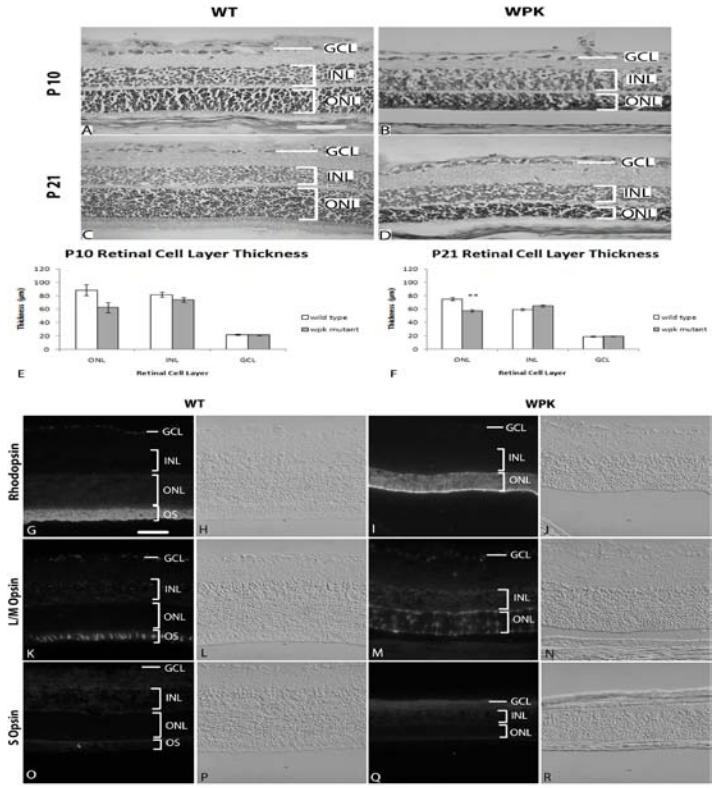

Figure 3.4 Retinal Cell Layer Thickness and Photoreceptors in *Mks3* Mutants. Retinal cell layer thickness was measured in sections through the central retinae 200µm dorsal and ventral to the optic nerve in WT at P10 (A) and P21 (C) and mutant P10 (B) and P21 (D). Graphs were made for P10 (E) and P21 (F) to compare the average thickness per sample of each retinal cell layer in WT and mutant retinae. At P10, no statistically significant changes in thickness occurred in any layer; however, there was already a decrease in the thickness of the outer nuclear layer (E). At P21, there were no significant changes in the inner and ganglion cell layers (F). However, there was a statistically significant change in the outer nuclear layer (**p<.001 two-tailed t-test). To determine the effect of *Mks3* mutation in photoreceptors at P21, sections were immunolabeled for rhodopsin (G, I), L/M opsin (K, M) and S opsin (O, Q). In WT retina, all opsins were localized to the photoreceptor outer segment, while in WPK mutant retina, expression of opsin expression was mislocalized to the photoreceptor cell body and synaptic regions. Nomarski optics is shown for each section (H, J, L, N, P and R). GCL, ganglion cell layer; INL, inner nuclear layer; ONL, outer nuclear layer; OS, outer segment. Scale bar: (A, G) 50µm.

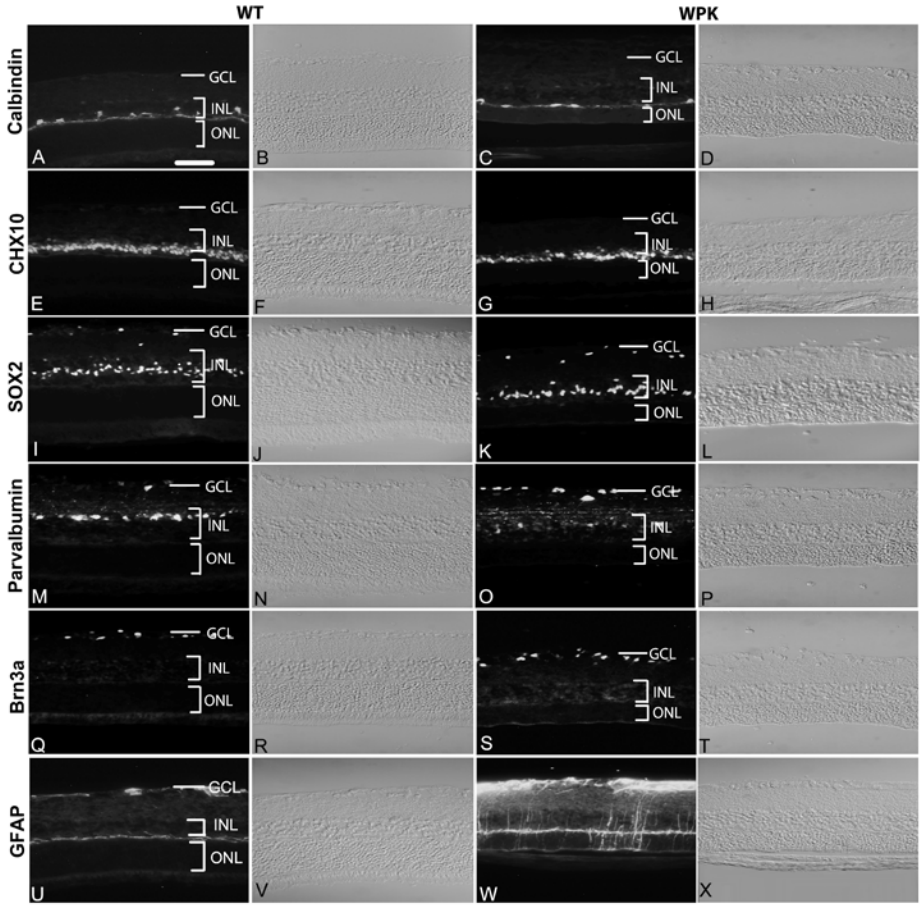

Figure 3.5 Cell-Type Specific Immunolabeling in the MKS3 Mutant Retina. Cell type-specific immunolabeling was performed using sections from both WT (A, E, I, M, Q, U) and *Mks3* mutant (C, G, K, O, S, W): horizontal cells were labeled with calbindin (A, C), bipolar cells with Chx10 (E, G), Muller glia cells with Sox2 (I, K), amacrine cells with parvalbumin (M, O), and ganglion cells with Brn3a (Q, S). Calbindin, Chx10, Sox2 and Brn3a positive cells were fairly similar in number in WT and mutant retinae. A similar number of parvalbumin + cells were found in both the WT and mutant retinae, but with a greater amount of those in the mutant were found in the GCL rather than the INL. Sections through WT (U) and mutant (W) retinae were labeled with glial fibrillary acidic protein to detect reactive glia present in degenerating retinae. There was little expression in the WT (U) at P21; however, there was a significant increase in the mutant (W). Nomarski optics for each section is shown in B, D, F, H, J, L, N, P, R, T, V and X. GCL, ganglion cell layer; INL, inner nuclear layer; ONL, outer nuclear layer. Scale bar: (A) 50µm.

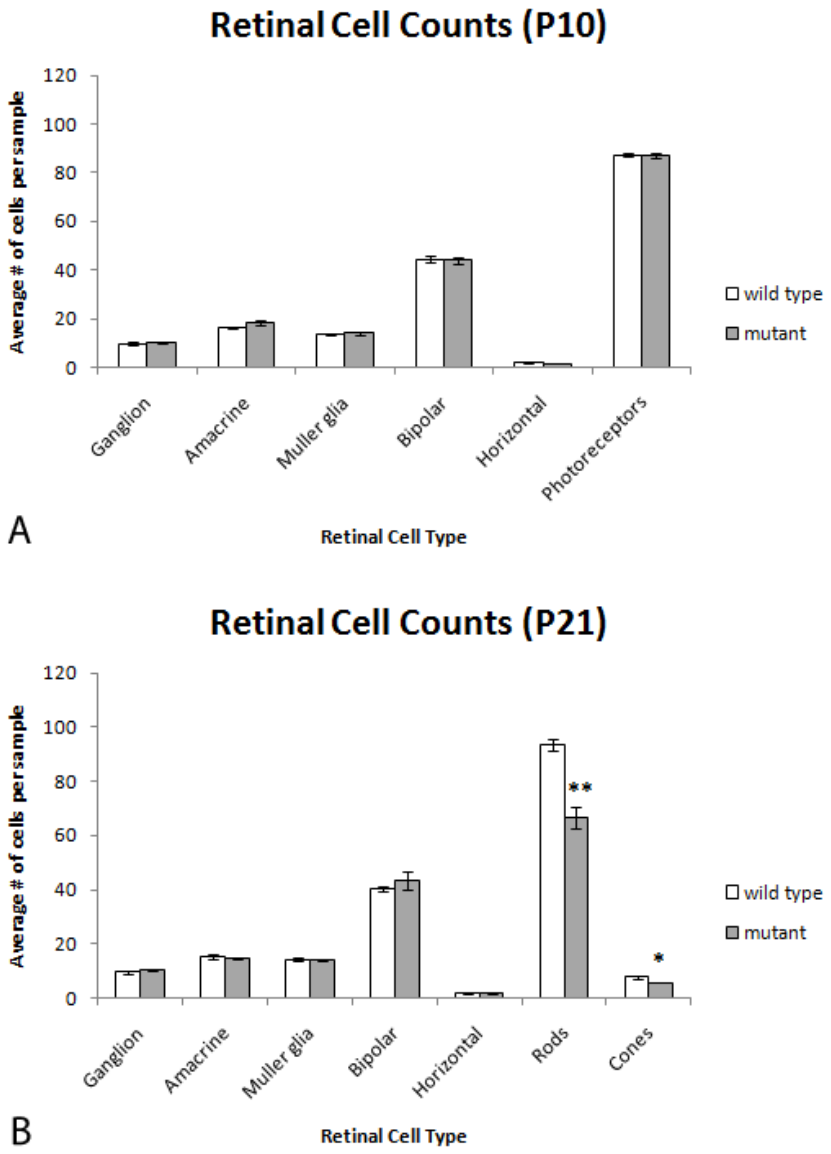

Figure 3.6 **Retinal Cell Counts.** Retinal cell counts were performed to compare the WT and mutant retinal cell counts at P10 and P21. At P10 (A), all retinal cell types present seem to be similar in both the WT and mutant rat retina. Photoreceptor cell types were significantly fewer in number in the mutant at P21 (B) when compared to the WT. All other cell types were similar.

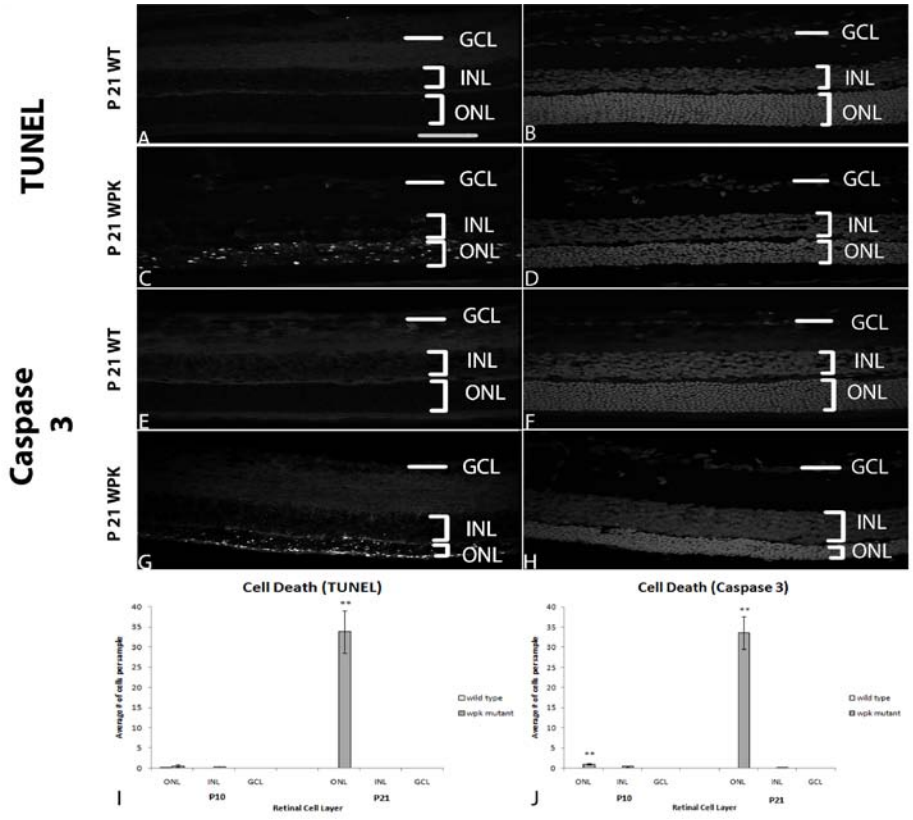

Figure 3.7 Cell Death of MKS3 Mutant Photoreceptors. The amount of cell death was observed by TUNEL and caspase labeled of the P21 WT (A, E) and P21 mutant (C, G) retinae. Hoechst staining is shown for each section in B, D, F and H. Both TUNEL and caspase 3 labels showed an abundance of cell death expression in the outer nuclear layer of the P21 mutant rat retinae in comparison to the WT. Graphs depict counts of cells positive for TUNEL (I) and caspase 3 (J) label in each of the retinal cell layers (n=3 retinae for each sample). There were no significant differences in the number of TUNEL (+) cells at P10; however, there was a large statistically significant increase in the number of TUNEL (+) cells at P21 ($p < 0.005$). No significant differences were noted in the WT and mutant INL and GCL at P10 and P21 using caspase 3. However, statistically significant increases in caspase 3-labeled cells were found in the ONL of the *Mks3* mutant in comparison to WT at both P10 and P21. (*$p < 0.01$ and **$p < 0.001$ respectively). GCL, ganglion cell layer; INL, inner nuclear layer; ONL, outer nuclear layer; OS, outer segment. Scale bar: (A) 50µm.

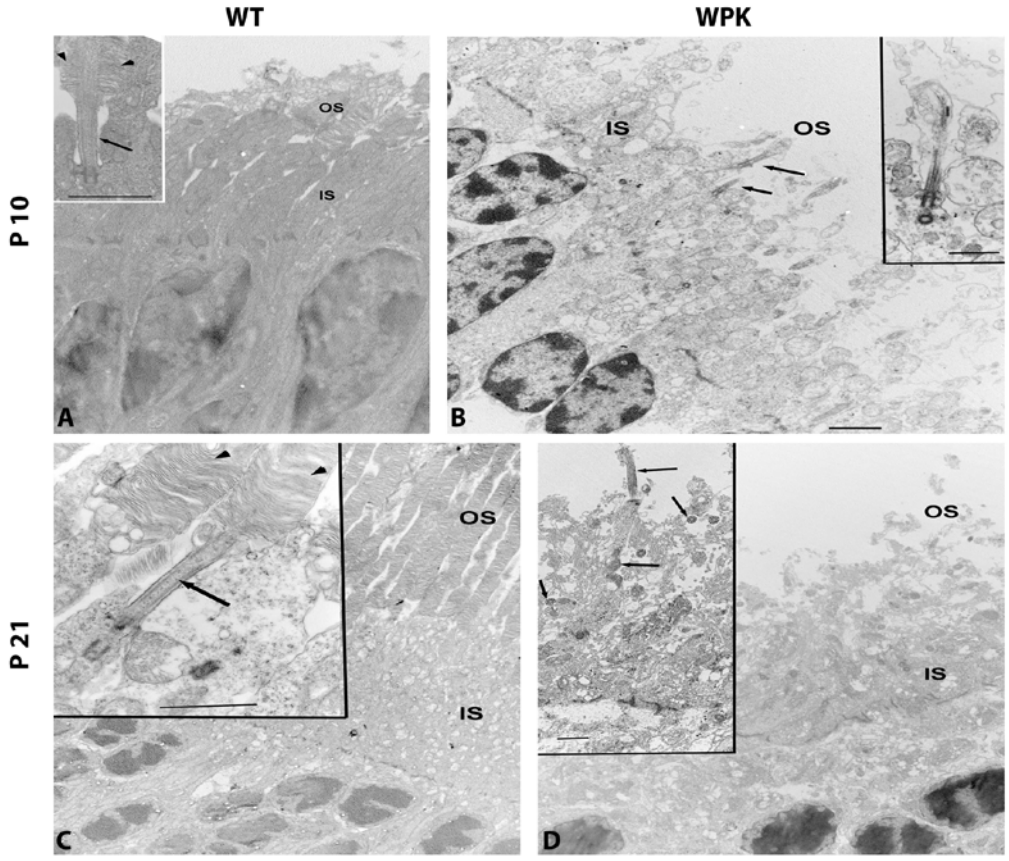

Figure 3.8 Electron Microscopy of Photoreceptor Outer Segments. Electron microscopy images were compared at P10 and P21 in WT (A & C) and mutant (B & D) retinae. The inner segment (IS) is connected to the outer segment (OS) by a connecting cilium (arrows) in both WT and mutant retinae. At P10, the beginning outer segment discs can be found (A inset, arrowhead) while in the mutant (B) cilia associated with a bulbous expansion without any discs were observed (B inset). At P21, the WT retina has a well developed OS with discs (C), while the mutant (D) demonstrates cilia extending into the OS space with some loosely associated membranous material, but no discs were observed.